



HAL
open science

Aerosol background concentrations influence aerosol-cloud interactions as much as the choice of aerosol-cloud parameterization

Louis Marelle, Gunnar Myhre, Jennie L Thomas, Jean-Christophe Raut

► To cite this version:

Louis Marelle, Gunnar Myhre, Jennie L Thomas, Jean-Christophe Raut. Aerosol background concentrations influence aerosol-cloud interactions as much as the choice of aerosol-cloud parameterization. 2024. insu-04693090

HAL Id: insu-04693090

<https://insu.hal.science/insu-04693090>

Preprint submitted on 10 Sep 2024

HAL is a multi-disciplinary open access archive for the deposit and dissemination of scientific research documents, whether they are published or not. The documents may come from teaching and research institutions in France or abroad, or from public or private research centers.

L'archive ouverte pluridisciplinaire **HAL**, est destinée au dépôt et à la diffusion de documents scientifiques de niveau recherche, publiés ou non, émanant des établissements d'enseignement et de recherche français ou étrangers, des laboratoires publics ou privés.

Aerosol background concentrations influence aerosol-cloud interactions as much as the choice of aerosol-cloud parameterization

Louis Marelle¹, Gunnar Myhre², Jennie L Thomas³, and Jean-Christophe Raut⁴

¹Laboratoire Atmospheres Milieux Observations Spatiales Site Paris-Jussieu

²CICERO, Norway

³L'Institut des Géosciences de l'Environnement (IGE)

⁴UPMC

August 22, 2024

Abstract

We use an independent observational estimate of aerosol-cloud interactions (ACI) during the 2014 Holuhraun volcanic eruption in Iceland to evaluate 4 ACI parameterizations in a regional model. All parameterizations reproduce the observed pattern of liquid cloud droplet size reduction during the eruption, but strongly differ on its magnitude and on the resulting effective radiative forcing (ERF). Our results contradict earlier findings that this eruption could be used to constrain liquid water path (LWP) adjustments in models, except to exclude extremely high LWP adjustments of more than 20 g/m². The modeled ERF is very sensitive to the non-volcanic background aerosol concentration: doubling the non-volcanic aerosol background weakens the ACI ERF by ~30%. Since aerosol biases in climate models can be an order of magnitude or more, these results suggest that aerosol background concentrations could be a major and under-examined source of uncertainty for modeling ACI.

Hosted file

Supplement_ACI_volcano.docx available at <https://authorea.com/users/564186/articles/1216636-aerosol-background-concentrations-influence-aerosol-cloud-interactions-as-much-as-the-choice-of-aerosol-cloud-parameterization>

1 **Aerosol background concentrations influence**
2 **aerosol-cloud interactions as much as the choice of**
3 **aerosol-cloud parameterization**

4 **Louis Marelle¹, Gunnar Myhre², Jennie L. Thomas³, Jean-Christophe Raut¹**

5 ¹Sorbonne Université, UVSQ, CNRS, LATMOS, Paris, France

6 ²Center for International Climate Research, Oslo, Norway

7 ³Université Grenoble Alpes, CNRS, IRD, Grenoble INP, IGE, Grenoble, France

8 **Key Points:**

- 9 • 4 aerosol-cloud parameterizations tested in a regional model are consistent with
10 observed cloud changes during the 2014 Holuhraun eruption
11 • Liquid water path (LWP) observations during the eruption are not enough to ex-
12 clude large LWP adjustments in models
13 • Aerosol radiative impacts are as sensitive to background aerosols as to aerosol-cloud
14 interactions parameterization choice

Corresponding author: Louis Marelle, louis.marelle@latmos.ipsl.fr

Abstract

We use an independent observational estimate of aerosol-cloud interactions (ACI) during the 2014 Holuhraun volcanic eruption in Iceland to evaluate 4 ACI parameterizations in a regional model. All parameterizations reproduce the observed pattern of liquid cloud droplet size reduction during the eruption, but strongly differ on its magnitude and on the resulting effective radiative forcing (ERF). Our results contradict earlier findings that this eruption could be used to constrain liquid water path (LWP) adjustments in models, except to exclude extremely high LWP adjustments of more than 20 g m^{-2} . The modeled ERF is very sensitive to the non-volcanic background aerosol concentration: doubling the non-volcanic aerosol background weakens the ACI ERF by $\sim 30\%$. Since aerosol biases in climate models can be an order of magnitude or more, these results suggest that aerosol background concentrations could be a major and under-examined source of uncertainty for modeling ACI.

Plain Language Summary

Particles suspended in the atmosphere (aerosols) play a key role in cloud formation. These aerosol-cloud interactions have a major but uncertain influence on climate. We compare 4 different ways to calculate aerosol-cloud interactions in a numerical atmospheric model. We compare model results to observed changes in clouds measured from satellites during the Holuhraun eruption in Iceland in 2014, which released large amounts of volcanic gases forming atmospheric aerosols. We find that all 4 approaches reproduce the observed reduction in cloud droplet sizes during the eruption, but that they disagree on its intensity and its impacts on the Earth's energy budget. An earlier study found that aerosol-cloud interactions did not significantly increase the amount of liquid water in the clouds; using a more recent version of the satellite observations we find that large increases are possible. We also show that the eruption's impacts on the Earth's energy budget strongly depend on non-volcanic aerosols already present in the atmosphere: doubling non-volcanic aerosols reduces the impacts by $\sim 30\%$. Aerosol biases in climate models can be far greater, indicating that this could be a major source of uncertainty for aerosol-cloud interactions and for understanding past, present and future climates.

1 Introduction

In Earth's atmosphere, a liquid cloud droplet can only form on a preexisting aerosol serving as a cloud condensation nucleus (CCN). As a result, the abundance and properties of aerosols have a direct influence on the physical and optical properties of clouds, and ultimately on the radiative budget of the Earth, through a range of processes called aerosol-cloud interactions (ACI, e.g. Lohmann & Feichter, 2005). The effective radiative forcing of ACI is currently estimated at -0.8 W m^{-2} , with likely values ranging from -1.45 to -0.25 W m^{-2} (IPCC, 2023). Despite the importance of ACI forcing for climate, this very wide uncertainty range has not been reduced significantly in recent years, and ACI remain the main source of uncertainty for quantifying anthropogenic radiative forcing, and a key physical uncertainty in climate projections.

Aerosols have a cooling effect on the global climate, but clean air policies have helped reduce aerosol pollution in recent years. There is evidence that improvements in air quality have also reduced aerosol cooling globally, revealing more of the underlying greenhouse gas warming trend (Quaas et al., 2022; Hodnebrog et al., 2024). In the Arctic, a region particularly sensitive to climate change, this "unmasking" of greenhouse warming may have been responsible for $+0.8^\circ\text{C}$ of additional warming from 1990 to 2015, half of the anthropogenic warming trend during the same period (von Salzen et al., 2022). These trends will likely continue in the future because of further emission reductions. In order to improve climate projections and to understand past changes, and to inform the policies that consider the trade-offs between short term and long term climate strate-

gies, it is thus critical to better constrain the ACI forcing and the main causes of uncertainty between models.

The impacts of ACI are hard to constrain in models because of the complexity of the processes involved, from the underlying microphysical changes to the interactions with cloud-scale and large-scale dynamics (e.g., Lohmann et al., 2016). To the first order, increasing aerosol concentrations increases liquid cloud droplet numbers and reduces cloud droplet size, forming optically thicker clouds than in aerosol-poor conditions (Twomey, 1974). In order to represent this process, climate models use ACI parameterizations of varying complexities, but it is unclear how much this range of parameterizations influences the predicted ACI radiative forcing uncertainty (Ekman, 2014), or how to best evaluate them against observations.

In fact, modeled ACI are also difficult to evaluate because the effects of ACI are very hard to observe directly. It is possible to compare observations of polluted clouds from unpolluted clouds, but attributing the differences to ACI requires very large datasets for controlling for all other causes of variability. Satellites could provide such a dataset, but they have limited sensitivity to cloud microphysics and are not currently able to estimate vertically resolved aerosol concentrations inside clouds (Quaas et al., 2020). Furthermore, due to the magnitude of anthropogenic and natural emissions of aerosols and their precursors, it is not feasible either to conduct controlled field experiments, such as emitting large enough amounts of aerosols during a long enough period. Large volcanic eruptions can be thought of as rare natural opportunistic experiments that can help us circumvent this problem (Christensen et al., 2022).

The Holuhraun fissure eruption in Iceland, from late August 2014 to February 2015, emitted the equivalent of 2 years of the European Union’s anthropogenic SO₂ emissions in just 6 months (Pfeffer et al., 2018; EEA, 2014), with most of the emissions occurring during the first two months of the eruption. During this time, observed cloud droplet sizes in the North Atlantic were reduced far outside the range of natural variability, due to ACI from volcanic aerosols. This independent observational estimate of ACI was compared previously to the predictions of climate models, showing that several models were inconsistent with observations (Malavelle et al., 2017).

In this study, we compare observed ACI in liquid clouds during the Holuhraun eruption against the predictions of 4 different ACI parameterizations in the same model framework. Specifically, we evaluate how well the different ACI parameterizations reproduce observed liquid cloud changes during the 2014 Holuhraun eruption, we quantify the uncertainty range in ACI radiative effect resulting from the choice of parameterization, and we compare this parameterization uncertainty to the uncertainty due to aerosol biases in the model. We show that the background aerosol concentration is a critical factor for modeling ACI accurately, and we discuss the wider implications for radiative forcing and climate modeling in the conclusion.

2 Methods

2.1 WRF-Chem 4.3.3 model

We perform simulations with the Weather Research and Forecasting model including chemistry (WRF-Chem, Grell et al., 2005), starting on 2014-08-15 and ending on 2014-11-01, allowing for 2 weeks of initial spin-up before the start of the eruption on 2014-08-29. The simulation domain is approximately 6000 km × 6000 km in size, and centered on Iceland. The horizontal resolution is 50 km × 50 km with 72 vertical levels between the surface and 50 hPa.

112 All simulations are performed with WRF-Chem version 4.3.3, including optimiza-
 113 tions for polar regions described in Marelle et al. (2017). New model updates since Marelle
 114 et al. (2017) are described below, including ACI developments presented in Section 2.1.4.

115 **2.1.1 WRF-Chem chemistry-aerosol setup**

116 Within WRF-Chem, we use the MOZART gas-phase chemistry mechanism (Emmons
 117 et al., 2010), and the MOSAIC-4bin sectional aerosol model (Zaveri et al., 2008) includ-
 118 ing aqueous chemistry (a setup called MOZART-MOSAIC-4BIN-AQ in WRF-Chem).
 119 Initial and time-varying boundary conditions for trace gases and aerosols are from the
 120 CAM-Chem model (Tilmes et al., 2022). For this study, we also update the dimethyl-
 121 sulfide (DMS) chemistry scheme in MOZART-MOSAIC-4bin-AQ to von Glasow and Crutzen
 122 (2004). The updated DMS mechanism includes MSA aerosols and the associated het-
 123 erogeneous chemistry. It was partly implemented in WRF-Chem for the CBM-Z and CRIMECH
 124 mechanisms by Archer-Nicholls et al. (2014); we include it fully in MOZART-MOSAIC-
 125 4BIN-AQ.

126 **2.1.2 WRF-Chem meteorological setup**

127 In our simulations, grid-scale cloud microphysics are modeled by the 2-moment Thomp-
 128 son Aerosol-Aware scheme (Thompson & Eidhammer, 2014), and subgrid clouds by the
 129 Grell-3 cumulus scheme (Grell & Dévényi, 2002). We modified the cloud fraction diag-
 130 nosis in WRF-Chem to follow Xu and Randall (1996). Initial and time-varying (6 hours)
 131 boundary conditions for meteorology are taken from the ERA5 reanalysis (Copernicus
 132 Climate Change Service, 2017), and spectral nudging to ERA5 is also applied for wind
 133 and temperature features over the 700 km scale. The full meteorological setup is pro-
 134 vided in Table S1.

135 **2.1.3 Emissions used in WRF-Chem simulations**

136 Daily varying volcanic SO₂ emissions and plume emission heights for the Holuhraun
 137 eruption are from Pfeffer et al. (2018). Emissions are injected in WRF-Chem as a uni-
 138 form source from the provided plume bottom altitude to plume top, at the location of
 139 the eruption (64.87°N, 16.84°W). 1% of SO₂ emissions are emitted as primary sulfate (Ilyinskaya
 140 et al., 2017).

141 Anthropogenic emissions are from the CAMSv4.2 inventory, applying sector-dependent
 142 daily and hourly emission variations and vertical profiles (Denier van der Gon et al., 2011;
 143 Archer-Nicholls et al., 2014). 3% of anthropogenic SO_x is emitted as primary sulfate (Alexander
 144 et al., 2009). Open biomass burning emissions are from FINNv1.5 (Wiedinmyer et al.,
 145 2014).

146 Natural sea spray emissions from open oceans follow Ioannidis et al. (2023) but do
 147 not include experimental emissions of marine organics. Dust emissions are included (Chin
 148 et al., 2002), but are very low in the domain. Terrestrial biogenic emissions are from MEGANv2.1
 149 (Guenther et al., 2012), and DMS emissions use the ocean climatology of Lana et al. (2011)
 150 with the sea-air flux from Nightingale et al. (2000).

151 **2.1.4 Aerosol-cloud parameterizations implemented and compared in WRF- 152 Chem**

153 We compare 4 aerosol-cloud interaction parameterizations in the WRF-Chem model:

- 154 • TE14: The ACI parameterization of the Thompson aerosol-aware cloud model (Thompson
 155 & Eidhammer, 2014) calculates cloud droplet formation based on the thermody-
 156 namical conditions in the clouds and 2 aerosol parameters, the water-friendly and

ice-friendly aerosol number concentrations. In the base version of the model, TE14 initializes these aerosol numbers from a fixed climatology. Here, TE14 uses aerosol numbers predicted by WRF-Chem. The water-friendly aerosol is set as the hydrophilic volume fraction (sulfate, nitrate, ammonium, sea salt, MSA) of the total WRF-Chem aerosol number in each size bin. To eliminate a source of variability between simulations, ice-friendly aerosol numbers are set to the fixed minimum model value of 5 L^{-1} . This is consistent with the negligible emission of ice-active volcanic dust in the eruption, and with the low ice nucleating particle numbers at high latitudes (Li et al., 2022).

- ARG02: The parameterization of Abdul-Razzak and Ghan (2002) calculates aerosol activation and cloud droplet numbers based on aerosol size, number, and hygroscopicity in each size bin. It was already included in the WRF-Chem chemistry code as part of the Morrison and Lin microphysics schemes. We reimplemented ARG02 into Thompson microphysics, consistently with TE14. For consistency, both TE14 and ARG02 include the same sub-grid distribution of updraft velocity from Ghan et al. (1997).
- BL95: The parameterization of Boucher and Lohmann (1995) predicts cloud droplet number concentrations as a function of accumulation-mode sulfate mass. We include it in WRF-Chem by overwriting the cloud droplet number passed by Thompson microphysics to the radiation code by the BL95-predicted value.
- LMDZ6: This parameterization, based on BL95, is used in the LMDZ6 climate model (Madeleine et al., 2020), and predicts cloud droplet number concentrations as a function of accumulation-mode soluble mass. The implementation is the same as in BL95, using the WRF-Chem mass of sulfate, ammonium, and sea salt. The LMDZ6 model does not include nitrate or MSA, so these were not used for the calculation.

By design, LMDZ6 and BL95 only represent the effect of aerosols on cloud droplet number and radiation, the so-called “first indirect effect” (Twomey, 1974), while ARG02 and TE14 are also able to represent microphysical adjustments of clouds to ACI, influencing precipitation, cloud dynamics and lifetime, and liquid water path, the “second indirect effect” (Albrecht, 1989).

For each of these 4 ACI parameterizations, we perform a control simulation (VOLC) that includes volcanic emissions, and a counterfactual simulation (noVOLC) without volcanic emissions, for a total of 8 simulations. The difference VOLC-noVOLC is used to estimate the effect of ACI due to volcanic aerosols. In order to further reduce differences between simulations, only the ARG02 simulation is run as a fully coupled WRF-Chem simulation with prognostic aerosols. TE14, LMDZ6 and BL95 aerosols are instead forced by the 3-hourly aerosol fields produced by ARG02. Furthermore, to remove the contribution of direct aerosol-radiation interactions (ARI) from the VOLC-noVOLC signal, all 8 simulations include simplified ARI from identical climatological aerosol fields (Tegen et al., 1997), instead of using prognostic WRF-Chem aerosols. This workflow also has the advantage of speeding up the calculations significantly, allowing for the sensitivity simulations presented in Section 3.4. But the main advantage is that all 4 ACI setups use the exact same meteorological setup, ARI, ice nucleation scheme, and aerosol fields for liquid cloud ACI, ensuring that the only difference between them is the choice of the liquid-cloud ACI parameterization.

2.2 MODIS observations of clouds for evaluating modeled ACI

We estimate the effect of the eruption on cloud properties using observations from the MODIS instruments on board of the Aqua and Terra satellites, using the $1^\circ \times 1^\circ$ monthly gridded cloud products MYD08_M3.6.1 and MOD08_M3.6.1. Specifically, we compute

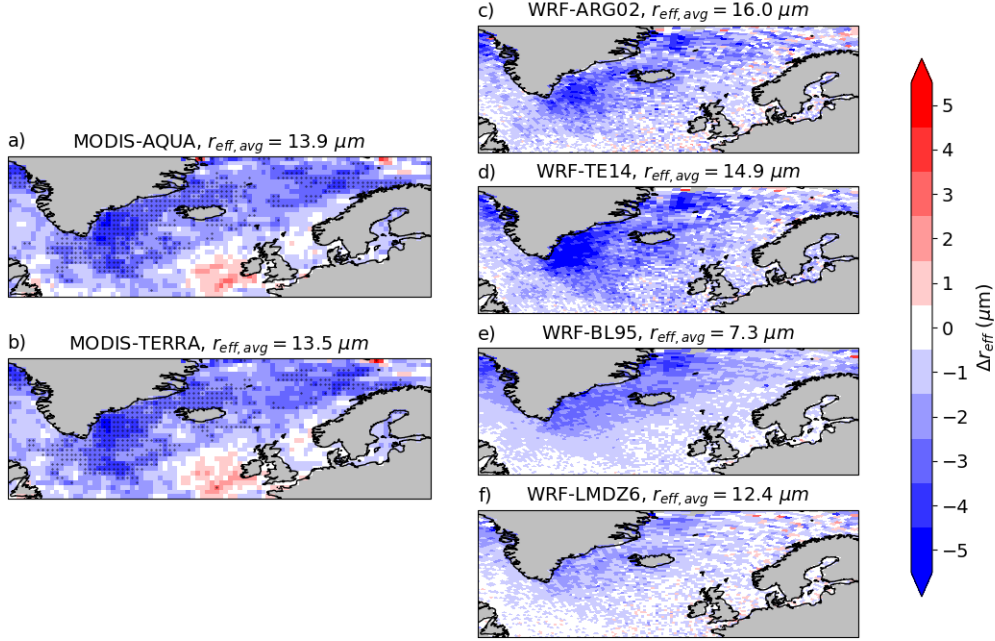


Figure 1. Cloud liquid droplet effective radius response to volcanic aerosols. a) MODIS-AQUA and b) MODIS-Terra liquid cloud droplet effective radius anomaly in October 2014, 2002-2022 baseline. c-d-e-f) WRF-Chem liquid cloud droplet effective radius anomaly due to volcanic emissions (VOLC - noVOLC anomaly, October 2014 average) using the c) ARG02 d) TE14 e) BL95 and f) LMDZ6 ACI parameterizations. Above each panel, $r_{eff,avg}$ gives the regionally averaged r_{eff} in October 2014, observed or modeled in the Volc simulation.

207 the October 2014 MODIS liquid effective radius (r_{eff}) and liquid water path (LWP) anomalies from the October 2002-2022 climatological baseline (excluding 2014).
208

209 For a like-for-like comparison of MODIS and WRF-Chem, WRF-Chem r_{eff} and
210 LWP are postprocessed to follow the MODIS monthly L3 product procedure (Hubanks
211 et al., 2016). Cloud properties are extracted from the 3-hourly WRF-Chem output, keep-
212 ing only daytime scenes with solar zenith angles less than 81.373° , producing daily maps,
213 which are then aggregated to monthly gridded maps of r_{eff} and LWP. MODIS in-cloud
214 LWP is compared with WRF-Chem’s grid-scale LWP by multiplying the in-cloud val-
215 ues with the liquid cloud fraction. Regionally averaged comparisons in Section 3 are taken
216 over ocean points only, from latitudes 47°N to 77°N , longitudes 60°W to 30°E , with area-
217 weighted averaging.

218 3 Results

219 3.1 Effect of the eruption on the cloud droplet radius, and sensitivity 220 to ACI parameterization

221 In October 2014, during the Holuhraun eruption, the MODIS cloud r_{eff} was sig-
222 nificantly smaller than usual. On average in the North Atlantic, the effective radius anomaly
223 $\Delta r_{eff} = -1.48\mu\text{m}$ (Figure 1), outside 2 standard deviations of the climatology ($2\sigma =$
224 $1.14\mu\text{m}$). This is a consequence of ACI from the additional volcanic aerosols (Malavelle
225 et al., 2017).

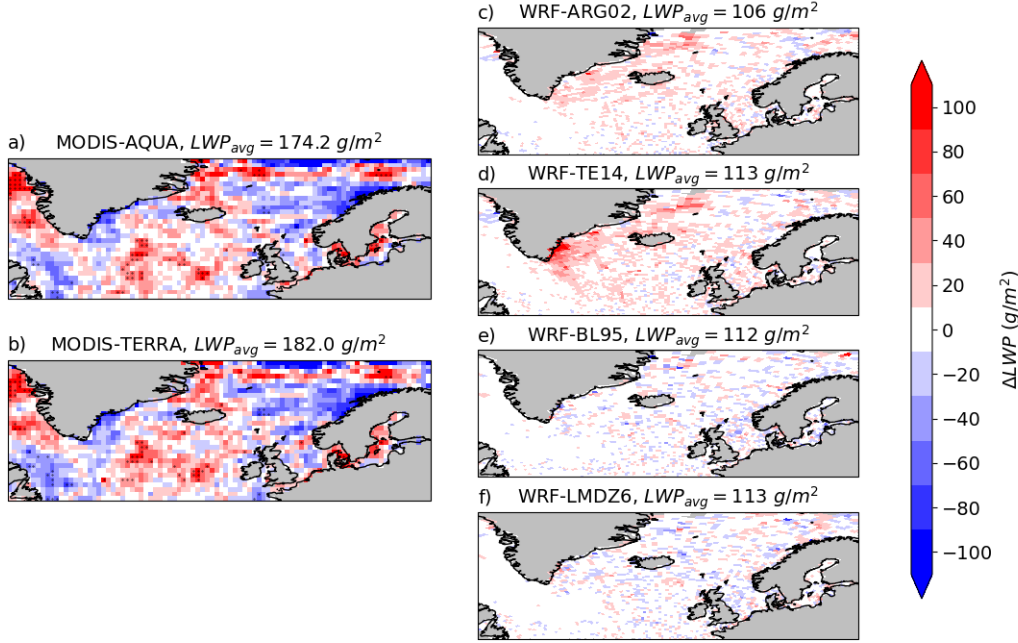


Figure 2. Liquid water path response to volcanic aerosols. a) MODIS-AQUA and b) MODIS-Terra liquid water path radius anomaly observed in October 2014, 2002-2022 baseline. c-d-e-f) WRF-Chem liquid water path anomaly due to volcanic emissions (VOLC - NOVOLC anomaly), October 2014 average, using the b) ARG02 c) TE14 d) BL95 and e) LMDZ6 ACI parameterizations. BL95 and LMDZ6 do not include the second indirect effect.

226 The 4 ACI parameterizations predict a strong r_{eff} reduction in the domain, and
 227 reproduce the overall geographical pattern of this change. The modeled Δr_{eff} is sensi-
 228 tive to the choice of ACI parameterization, with $-1.20 \mu m$, $-1.63 \mu m$, $-1.09 \mu m$ and $-$
 229 $0.66 \mu m$ for ARG02, TE14, BL95, and LMDZ6 respectively (Table S2). The simple BL95
 230 parameterization predicts a reasonable Δr_{eff} anomaly, but strongly underestimates the
 231 observed absolute r_{eff} by -47% . Conversely, LMDZ6 reproduces the observed r_{eff} but
 232 strongly underestimates the observed Δr_{eff} by -55% . Implications for radiative forcing
 233 in LMDZ6 are discussed in Section 3.3.

234 3 of the 4 parameterizations underestimate Δr_{eff} . This could be a limitation of
 235 the ACI parameterizations themselves, or it could be due to underestimated aerosols in
 236 the volcanic plume. During the eruption, the WRF-ARG02 simulation reproduces the
 237 observations of fine particle mass concentration ($PM_{2.5}$) at European surface sites very
 238 well (Figure S1a). Before the start of the eruption, background aerosol sulfate is also well
 239 represented, but after the eruption begins in late August, the model underestimates sul-
 240 fate at surface sites (Figure S1b). To our knowledge, the vertical distribution of aerosols
 241 in the Holuhraun plume was not observed, so it is not clear if the same bias is present
 242 at higher altitudes where aerosols interact with clouds, or if it could be due to errors in
 243 the downward mixing of the volcanic plume into the boundary layer. In the following,
 244 we will focus on the sensitivity of ACI to parameterizations and aerosols in the model.

3.2 Effect of the eruption on the liquid water path, and sensitivity to ACI parameterization

Figure 2 compares the observed and modeled LWP anomaly due to the eruption in October 2014. WRF-ARG02 and WRF-TE14 show a weak regionally-averaged ΔLWP response of $+3.9 \text{ g m}^{-2}$ and $+6.8 \text{ g m}^{-2}$ respectively (Table S2), well below the threshold of observed natural variability ($2\sigma = 19.3 \text{ g m}^{-2}$). It is important to note that BL95 and LMDZ6 do not include cloud microphysical adjustments to the r_{eff} change (the second indirect effect). For BL95 and LMDZ6, LWP changes are then only due to random variability and small dynamical adjustments to the first indirect effect, and are as expected close to zero. The absolute regionally-averaged LWP is close to 110 g m^{-2} with all parameterizations, significantly lower than MODIS observations ($\sim 180 \text{ g m}^{-2}$), but higher than the climate model simulations in Malavelle et al. (2017) (mean LWP $\sim 60 \text{ g m}^{-2}$).

Using MODIS products from version 5.1, Malavelle et al. (2017) found that the impact of the eruption on LWP was very limited, and could not exceed 9 g m^{-2} . They concluded that large LWP adjustments in climate models were inconsistent with these observations. Using revised LWP from MODIS version 6.1, and a longer climatological period (2002-2022 excluding 2014 instead of 2002-2013) we find a much larger significance threshold $2\sigma = 19.3 \text{ g m}^{-2}$, which is consistent with even the largest climate model ΔLWP of 16.3 g m^{-2} from Malavelle et al. (2017).

A recent study suggested that the cloud response to the Holuhraun eruption could be dominated by cloud fraction adjustment, instead of changes in LWP or r_{eff} (Chen et al., 2022). This is not the case here, and WRF-ARG02 and WRF-TE14 predict positive but very small cloud fraction adjustments of $+0.4$ and $+0.8$ percentage points respectively (Figure S2 and Table S2).

3.3 Sensitivity of the aerosol radiative impact to the ACI parameterization

The regionally averaged radiative effect of ACI on the net shortwave flux at top-of-atmosphere (ERF_{aci}^{SW}) in October 2014 is -1.12 , -1.97 , -1.08 and -0.34 W m^{-2} for ARG02, TE14, BL95, and LMDZ6 respectively (Table S2). The weak -0.34 W m^{-2} ERF_{aci}^{SW} in LMDZ6 is consistent with its low Δr_{eff} response. This could explain why the IPSL-CM6 climate model, where LMDZ6 is hosted, has the weakest ACI effective radiative forcing among CMIP6 models (Zelinka et al., 2023). Despite very different approaches and complexities, ARG02 and BL95 predict a similar ERF_{aci}^{SW} . TE14, which best reproduces the observed r_{eff} and Δr_{eff} , also predicts the strongest forcing, nearly 2 times stronger than ARG02 and BL95.

3.4 Sensitivity of the modeled cloud response to the aerosol background

Aerosol-cloud interactions are strongly non-linear. For this reason, the modeled radiative impact of an aerosol perturbation is sensitive to the absolute aerosol concentrations in the background state (Carslaw et al., 2013; Lohmann et al., 2000). In order to estimate the sensitivity of the modeled ACI to the non-volcanic aerosol background, we perform sensitivity experiments in the WRF-Chem model by perturbing the non-volcanic aerosol climatology aer (units $\mu\text{g kg}^{-1}$ and kg^{-1}) used to force the TE14, LMDZ6, and BL95 parameterizations by a factor $\alpha = 0.5, 0.75, 1.5, \text{ or } 2$.

$$aer_{NoVolc,perturbed} = \alpha \times aer_{NoVolc} \quad (1)$$

$$aer_{Volc,perturbed} = \alpha \times aer_{NoVolc} + (aer_{Volc} - aer_{NoVolc}) \quad (2)$$

For each sensitivity simulation, we calculate the VOLC-noVOLC Δr_{eff} and ERF_{aci}^{SW} and compare it to the value from the unperturbed reference run, as a function of the perturbation anomaly $\alpha - 1.0$, which is equal to zero for the unperturbed case. Aerosols

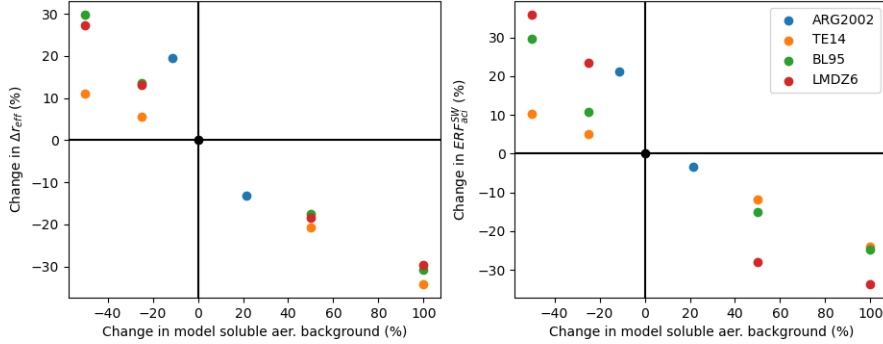


Figure 3. Sensitivity of volcanic aerosol-cloud-interactions to the non-volcanic aerosol background concentration. (left) effective radius anomaly during the eruption (right) indirect short-wave radiative effect of the eruption at top-of-atmosphere. All values are given as percentage changes from the unperturbed reference simulations.

292 cannot be perturbed directly in ARG02, because they are not forced but computed prog-
 293 nostically in the model. In order to estimate the sensitivity of ARG02 to background aerosol
 294 concentrations, we perturb instead the marine emissions of sea spray and DMS. Since
 295 these sensitivity simulations are fully coupled, they are computationally costly, and we
 296 only perform 2 sensitivity simulations with emissions multiplied by 0.5 and 2.

297 Figure 3 shows that the droplet effective radius and the aerosol forcing are very sen-
 298 sitive to the non-volcanic aerosol background. When the background aerosol concentra-
 299 tion is doubled (+100%), the Δr_{eff} is ~ 30 to 35% weaker than in the reference run, and
 300 the ERF_{aci}^{SW} is ~ 25 to 35% weaker, even though the volcanic aerosol perturbation is ex-
 301 actly the same. When the background is divided by 2 (-50%), the Δr_{eff} is ~ 10 to 30%
 302 stronger than in the reference run, and the ERF_{aci}^{SW} is ~ 10 to 40% larger. Since local
 303 biases in aerosol background concentrations can often be an order of magnitude or more
 304 in climate models (e.g. Lapere et al., 2023; Bian et al., 2024), this effect could be a major
 305 source of uncertainty for radiative forcing calculations.

306 4 Discussion, conclusions, and recommendations for climate model- 307 ing

308 In this study, we compare 4 ACI parameterizations in the same regional modeling
 309 framework during a large volcanic eruption. We calculate the sensitivity of the cloud re-
 310 sponse and the aerosol radiative forcing to the choice of parameterization, and the sensi-
 311 tivity of volcanic ACI to the non-volcanic aerosol background.

312 All 4 ACI parameterizations reproduce the pattern and overall magnitude of the
 313 observed change in liquid cloud droplet effective radius during the eruption, but LMDZ6
 314 underestimates this change. Modeled ACI are sensitive to ACI parameterization in terms
 315 of effective radius and radiative impacts. The ACI radiative impact is very weak for the
 316 LMDZ6 ACI parameterization, and we believe that this choice of parameterization could
 317 explain the low aerosol ERF in the associated IPSL-CM6 climate model. We did not test
 318 the full parameterization panel from CMIP6 models, and our results certainly underes-
 319 timate the full range of sensitivity to ACI parameterization; however, the types of pa-
 320 rameterizations tested are representative of this generation of climate models.

321 Our study disagrees with one of the main conclusions of Malavelle et al. (2017):
322 we find that this volcanic case study cannot be used to constrain the ACI LWP adjust-
323 ment in climate models, except to rule out very high regional LWP changes of more than
324 $\sim 20 \text{ g m}^{-2}$. These values are much larger than the magnitude of the LWP change due
325 to ACI in WRF-Chem in either ARG02 or TE14 ($\sim 5 \text{ g m}^{-2}$), and consistent with even
326 the largest LWP changes predicted by climate models in Malavelle et al. (2017). Our sim-
327 ulations and those of Malavelle et al. (2017) underestimate the observed LWP in the re-
328 gion, so further work is needed to fully understand LWP adjustments in models.

329 We find that the modeled cloud response to the eruption is also very sensitive to
330 the non-volcanic background aerosol concentration: a doubling of the aerosol background
331 translates into a $\sim -30\%$ change in ACI radiative forcing. This sensitivity is worrying
332 because biases in aerosol mixing ratio in climate models can be far greater. Allen and
333 Landuyt (2014) found that model spread for black carbon aerosols in CMIP5 is up to
334 2 orders of magnitude in the free troposphere, and Lapere et al. (2023); Bian et al. (2024)
335 showed that aerosol differences between models in the remote marine and polar tropo-
336 sphere, respectively, can be 1 or 2 orders of magnitude.

337 Nearly 25 years ago, Lohmann et al. (2000) showed that aerosol-cloud radiative forc-
338 ing in the ECHAM4 climate model was sensitive to the pre-industrial aerosol burden.
339 Based on this result, Lohmann and Feichter (2005) suggested that the large differences
340 in ERF_{ACI} between models could be due to “the dependence of the indirect aerosol ef-
341 fect on the background aerosol concentration”. Carslaw et al. (2013) later found that
342 uncertainties in natural emissions could account for 45% of the ERF_{ACI} uncertainty in
343 a single global model. However, to our knowledge, the precise contribution of these er-
344 rors to the large CMIP multimodel RF_{ACI} uncertainty has not been investigated since,
345 and was not identified as a major issue in recent efforts for understanding aerosol ERF
346 (Fiedler et al., 2023; Bellouin et al., 2020; Quaas et al., 2020; Mülmenstädt & Feingold,
347 2018; Seinfeld et al., 2016). In light of our results and of earlier literature, we recommend
348 a systematic analysis of how the natural aerosol background influences the ERF_{ACI} spread
349 in climate models. If background aerosols are indeed important, improving the repre-
350 sentation of natural aerosols such as sea-spray, sulfate from oceanic DMS, and biomass
351 burning could be a more efficient pathway for reducing ACI uncertainties than difficult
352 improvements in complex aerosol-cloud processes.

353 For this purpose, a detailed evaluation of aerosols in climate models is critical. ACI
354 are determined by aerosol properties within clouds, and are especially sensitive to aerosol
355 concentrations and aerosol size (Dusek et al., 2006). However, aerosols in climate mod-
356 els are usually evaluated in terms of vertically integrated bulk properties such as Aerosol
357 Optical Depth (AOD), which is also the usual CCN proxy for observational estimates
358 of the aerosol ERF (Bellouin et al., 2020; Gryspeerdt et al., 2023). This is concerning,
359 because large errors in aerosol concentrations, vertical distributions, water uptake, and
360 size distributions can compensate to give a reasonable AOD in models (Quaas et al., 2020).
361 In this context, we also recommend routine evaluations and comparisons of aerosol ver-
362 tical distributions in climate models, for example using the now extensive LiDAR and
363 aircraft measurement datasets.

364 The sensitivity of ACI to aerosol background is not just important in the pre-industrial
365 period and for quantifying ERF_{ACI} in climate models, which has been the focus until
366 now. Our results suggest that tackling these issues and improving the representation of
367 background aerosols in models could also help us better understand the effect of ACI at
368 shorter time scales, including the influence of ACI on specific extreme events, its effect
369 on meteorological forecasts, and the effect of recent and future clean air policies on cli-
370 mate.

Open Research Section

The updated WRF-Chem 4.3.3 model version used in this study can be found at <https://doi.org/10.5281/zenodo.12544534>. The WRF preprocessing system (WPS) is available at <https://archive.softwareheritage.org/swh:1:dir:21227ff84043afa53bb870245da4061fe7f0c7ab;origin=https://github.com/wrf-model/WPS;visit=swh:1:snp:096256316e752343901abad92a7dd9c2529f48cb;anchor=swh:1:rev:5a2ae63988e632405a4504cfb143ce7f0230a7a0>. WRF-Chem preprocessor tools (mozbc, fire_emiss and bio_emiss) are available at <https://www2.acom.ucar.edu/wrf-chem/wrf-chem-tools-community>. WRF-Chem run and setup scripts, preprocessing codes, and post-processing codes created for this study can be found at <https://doi.org/10.5281/zenodo.12544354>.

ERA5 input data on pressure and surface levels for WRF can be obtained at <https://doi.org/10.24381/cds.143582cf>. CAM-Chem input data for initial and boundary conditions is available at <https://doi.org/10.5065/NMP7-EP60..> CAMSv4.2 emissions are available at <https://ads.atmosphere.copernicus.eu/cdsapp#!/dataset/cams-global-emission-inventories> FINNv1.5 emissions are distributed at <https://www.acom.ucar.edu/Data/fire/>. The Lana DMS climatology can be found at https://www.bodc.ac.uk/solas_integration/implementation_products/group1/dms/documents/dmsclimatology.zip.

MODIS satellite observations from the MYD08_M3_6_1 and MOD08_M3_6_1 products can be retrieved from https://doi.org/10.5067/MODIS/MYD08_M3_061 and https://doi.org/10.5067/MODIS/MOD08_M3_061. Observations of atmospheric composition used in the supplement are from <https://ebas.nilu.no/>.

Acknowledgments

This project has received funding from Horizon Europe programme under Grant Agreement No 101137680 via project CERTAINTY (Cloud-aERosol inTeractions & their impActs IN The earth sYstem); from the European Union's Horizon 2020 research and innovation programme under Grant agreement No 101003826 via project CRiceS (Climate Relevant interactions and feedbacks: the key role of sea ice and Snow in the polar and global climate system); and from the project SUPER (no. 250573) funded through the Research Council of Norway. This research has been partly funded by French National Research Agency (ANR) via the project MPC2 (n° ANR-22-CEA01-0009-02). Computer analyses benefited from access to IDRIS HPC resources (GENCI allocations A011017141 and A013017141), and from the IPSL mesocenter ESPRI facility which is supported by CNRS, UPMC, Labex L-IPSL, CNES and Ecole Polytechnique. We acknowledge use of the WRF-Chem preprocessor tools mozbc, fire_emiss and bio_emiss provided by the Atmospheric Chemistry Observations and Modeling Lab (ACOM) of NCAR. We acknowledge ECCAD for the archiving and distribution of the CAMS emissions data.

References

- Abdul-Razzak, H., & Ghan, S. J. (2002). A parameterization of aerosol activation 3. sectional representation. *Journal of Geophysical Research: Atmospheres*, 107(D3), AAC 1-1-AAC 1-6. Retrieved from <https://agupubs.onlinelibrary.wiley.com/doi/abs/10.1029/2001JD000483> doi: <https://doi.org/10.1029/2001JD000483>
- Albrecht, B. A. (1989, September). Aerosols, Cloud Microphysics, and Fractional Cloudiness. *Science*, 245(4923), 1227–1230. Retrieved 2024-03-19, from <https://www.science.org/doi/10.1126/science.245.4923.1227> (Publisher: American Association for the Advancement of Science) doi: [10.1126/science.245.4923.1227](https://doi.org/10.1126/science.245.4923.1227)

- 420 Alexander, B., Park, R. J., Jacob, D. J., & Gong, S. (2009). Transition metal-
 421 catalyzed oxidation of atmospheric sulfur: Global implications for the sulfur
 422 budget. *Journal of Geophysical Research: Atmospheres*, *114*(D2). Retrieved
 423 from [https://agupubs.onlinelibrary.wiley.com/doi/abs/10.1029/](https://agupubs.onlinelibrary.wiley.com/doi/abs/10.1029/2008JD010486)
 424 [2008JD010486](https://doi.org/10.1029/2008JD010486) doi: <https://doi.org/10.1029/2008JD010486>
- 425 Allen, R. J., & Landuyt, W. (2014). The vertical distribution of black carbon in
 426 cmip5 models: Comparison to observations and the importance of convective
 427 transport. *Journal of Geophysical Research: Atmospheres*, *119*(8), 4808–4835.
 428 Retrieved from [https://agupubs.onlinelibrary.wiley.com/doi/abs/](https://agupubs.onlinelibrary.wiley.com/doi/abs/10.1002/2014JD021595)
 429 [10.1002/2014JD021595](https://doi.org/10.1002/2014JD021595) doi: <https://doi.org/10.1002/2014JD021595>
- 430 Archer-Nicholls, S., Lowe, D., Utembe, S., Allan, J., Zaveri, R. A., Fast, J. D.,
 431 ... McFiggans, G. (2014). Gaseous chemistry and aerosol mecha-
 432 nism developments for version 3.5.1 of the online regional model, wrf-
 433 chem. *Geoscientific Model Development*, *7*(6), 2557–2579. Retrieved
 434 from <https://gmd.copernicus.org/articles/7/2557/2014/> doi:
 435 [10.5194/gmd-7-2557-2014](https://doi.org/10.5194/gmd-7-2557-2014)
- 436 Bellouin, N., Quaas, J., Gryspeerdt, E., Kinne, S., Stier, P., Watson-Parris, D.,
 437 ... Stevens, B. (2020). Bounding global aerosol radiative forcing of
 438 climate change. *Reviews of Geophysics*, *58*(1), e2019RG000660. Re-
 439 trieved from [https://agupubs.onlinelibrary.wiley.com/doi/abs/](https://agupubs.onlinelibrary.wiley.com/doi/abs/10.1029/2019RG000660)
 440 [10.1029/2019RG000660](https://doi.org/10.1029/2019RG000660) (e2019RG000660 10.1029/2019RG000660) doi:
 441 <https://doi.org/10.1029/2019RG000660>
- 442 Bian, H., Chin, M., Colarco, P. R., Apel, E. C., Blake, D. R., Froyd, K., ... Zhu,
 443 J. (2024). Observationally constrained analysis of sulfur cycle in the ma-
 444 rine atmosphere with nasa atom measurements and aerocom model simula-
 445 tions. *Atmospheric Chemistry and Physics*, *24*(3), 1717–1741. Retrieved
 446 from <https://acp.copernicus.org/articles/24/1717/2024/> doi:
 447 [10.5194/acp-24-1717-2024](https://doi.org/10.5194/acp-24-1717-2024)
- 448 Boucher, O., & Lohmann, U. (1995, Jan). The sulfate-ccn-cloud albedo effect: A
 449 sensitivity study with two general circulation models. *Tellus B: Chemical and*
 450 *Physical Meteorology*. doi: [10.3402/tellusb.v47i3.16048](https://doi.org/10.3402/tellusb.v47i3.16048)
- 451 Carslaw, K. S., Lee, L. A., Reddington, C. L., Pringle, K. J., Rap, A., Forster,
 452 P. M., ... Pierce, J. R. (2013, November). Large contribution of natural
 453 aerosols to uncertainty in indirect forcing. *Nature*, *503*(7474), 67–71. Re-
 454 trieved 2024-04-18, from <https://www.nature.com/articles/nature12674>
 455 (Publisher: Nature Publishing Group) doi: [10.1038/nature12674](https://doi.org/10.1038/nature12674)
- 456 Chen, Y., Haywood, J., Wang, Y., Malavelle, F., Jordan, G., Partridge, D., ...
 457 Lohmann, U. (2022, August). Machine learning reveals climate forcing from
 458 aerosols is dominated by increased cloud cover. *Nature Geoscience*, *15*(8),
 459 609–614. Retrieved from <https://doi.org/10.1038/s41561-022-00991-6>
 460 doi: [10.1038/s41561-022-00991-6](https://doi.org/10.1038/s41561-022-00991-6)
- 461 Chin, M., Ginoux, P., Kinne, S., Torres, O., Holben, B. N., Duncan, B. N., ...
 462 Nakajima, T. (2002). Tropospheric aerosol optical thickness from the
 463 gocart model and comparisons with satellite and sun photometer mea-
 464 surements. *J. Atmos. Sci.*, *59*(3), 461–483. Retrieved from [http://](http://dx.doi.org/10.1175/1520-0469(2002)059<0461:TAOTFT>2.0.CO;2)
 465 [dx.doi.org/10.1175/1520-0469\(2002\)059<0461:TAOTFT>2.0.CO;2](http://dx.doi.org/10.1175/1520-0469(2002)059<0461:TAOTFT>2.0.CO;2) doi:
 466 [10.1175/1520-0469\(2002\)059<0461:TAOTFT>2.0.CO;2](https://doi.org/10.1175/1520-0469(2002)059<0461:TAOTFT>2.0.CO;2)
- 467 Christensen, M. W., Gettelman, A., Cermak, J., Dagan, G., Diamond, M., Douglas,
 468 A., ... Yuan, T. (2022). Opportunistic experiments to constrain aerosol ef-
 469 fective radiative forcing. *Atmospheric Chemistry and Physics*, *22*(1), 641–674.
 470 Retrieved from <https://acp.copernicus.org/articles/22/641/2022/> doi:
 471 [10.5194/acp-22-641-2022](https://doi.org/10.5194/acp-22-641-2022)
- 472 Copernicus Climate Change Service. (2017). *ERA5: Fifth generation of ECMWF at-*
 473 *mospheric reanalyses of the global climate*. Retrieved from [http://doi.org/](http://doi.org/10.24381/cds.adbb2d47)
 474 [10.24381/cds.adbb2d47](https://doi.org/10.24381/cds.adbb2d47) (Copernicus Climate Change Service Climate Data

- 475 Store (CDS), last accessed May 11th 2021)
- 476 Denier van der Gon, H., Hendriks, C., Kuenen, J., Segers, A. A., & Visschedijk, A.
477 (2011). *Description of current temporal emission patterns and sensitivity of*
478 *predicted AQ for temporal emission patterns, TNO Report, EU FP7 MACC de-*
479 *liverable report D_DEMIS-1.3* (Tech. Rep.). Princetonlaan 6, 3584 CB Utrecht,
480 The Netherlands: TNO.
- 481 Dusek, U., Frank, G. P., Hildebrandt, L., Curtius, J., Schneider, J., Walter, S., ...
482 Andreae, M. O. (2006). Size matters more than chemistry for cloud-nucleating
483 ability of aerosol particles. *Science*, *312*(5778), 1375-1378. Retrieved from
484 <https://www.science.org/doi/abs/10.1126/science.1125261> doi:
485 10.1126/science.1125261
- 486 EEA. (2014). *Emission trends of sulphur oxides* [Data Visualization]. Retrieved
487 2024-04-17, from https://www.eea.europa.eu/data-and-maps/daviz/emission-trends-of-sulphur-oxides#tab-chart_1
- 488 Ekman, A. M. L. (2014). Do sophisticated parameterizations of aerosol-
489 cloud interactions in CMIP5 models improve the representation of re-
490 cent observed temperature trends? *Journal of Geophysical Research:*
491 *Atmospheres*, *119*(2), 817–832. Retrieved 2024-04-17, from <https://onlinelibrary.wiley.com/doi/abs/10.1002/2013JD020511> (eprint:
492 <https://onlinelibrary.wiley.com/doi/pdf/10.1002/2013JD020511>) doi:
493 10.1002/2013JD020511
- 494 Emmons, L. K., Walters, S., Hess, P. G., Lamarque, J.-F., Pfister, G. G., Fillmore,
495 D., ... Kloster, S. (2010). Description and evaluation of the Model for Ozone
496 and Related chemical Tracers, version 4 (MOZART-4). *Geoscientific Model*
497 *Development*, *3*(1), 43–67. doi: 10.5194/gmd-3-43-2010
- 498 Fiedler, S., van Noije, T., Smith, C. J., Boucher, O., Dufresne, J.-L., Kirkevåg, A.,
499 ... Schulz, M. (2023). Historical changes and reasons for model differences in
500 anthropogenic aerosol forcing in cmip6. *Geophysical Research Letters*, *50*(15),
501 e2023GL104848. Retrieved from [https://agupubs.onlinelibrary.wiley](https://agupubs.onlinelibrary.wiley.com/doi/abs/10.1029/2023GL104848)
502 [.com/doi/abs/10.1029/2023GL104848](https://agupubs.onlinelibrary.wiley.com/doi/abs/10.1029/2023GL104848) (e2023GL104848 2023GL104848) doi:
503 <https://doi.org/10.1029/2023GL104848>
- 504 Ghan, S. J., Leung, L. R., Easter, R. C., & Abdul-Razzak, H. (1997). Prediction
505 of cloud droplet number in a general circulation model. *Journal of Geophysi-*
506 *cal Research: Atmospheres*, *102*(D18), 21777-21794. Retrieved from <https://agupubs.onlinelibrary.wiley.com/doi/abs/10.1029/97JD01810> doi:
507 <https://doi.org/10.1029/97JD01810>
- 508 Grell, G. A., & Dévényi, D. (2002). A generalized approach to parameterizing con-
509 vection combining ensemble and data assimilation techniques. *Geophysical Re-*
510 *search Letters*, *29*(14), 38–1–38–4. doi: 10.1029/2002GL015311
- 511 Grell, G. A., Peckham, S. E., Schmitz, R., McKeen, S. A., Frost, G., Skamarock,
512 W. C., & Eder, B. (2005). Fully coupled “online” chemistry within
513 the wrf model. *Atmospheric Environment*, *39*(37), 6957-6975. Re-
514 trievied from <https://www.sciencedirect.com/science/article/pii/S1352231005003560> doi: <https://doi.org/10.1016/j.atmosenv.2005.04.027>
- 515 Gryspereidt, E., Povey, A. C., Grainger, R. G., Hasekamp, O., Hsu, N. C., Mulcahy,
516 J. P., ... Sorooshian, A. (2023). Uncertainty in aerosol–cloud radiative forcing
517 is driven by clean conditions. *Atmospheric Chemistry and Physics*, *23*(7),
518 4115–4122. Retrieved from [https://acp.copernicus.org/articles/23/](https://acp.copernicus.org/articles/23/4115/2023/)
519 [4115/2023/](https://acp.copernicus.org/articles/23/4115/2023/) doi: 10.5194/acp-23-4115-2023
- 520 Guenther, A. B., Jiang, X., Heald, C. L., Sakulyanontvittaya, T., Duhl, T., Em-
521 mons, L. K., & Wang, X. (2012). The Model of Emissions of Gases and
522 Aerosols from Nature version 2.1 (MEGAN2.1): an extended and updated
523 framework for modeling biogenic emissions. *Geoscientific Model Development*,
524 *5*(6), 1471–1492. doi: 10.5194/gmd-5-1471-2012
- 525 Hodnebrog, O., Myhre, G., Jouan, C., Andrews, T., Forster, P. M., Jia, H., ...

- 530 Schulz, M. (2024, April). Recent reductions in aerosol emissions have
 531 increased Earth’s energy imbalance. *Communications Earth & Environ-*
 532 *ment*, 5(1), 1–9. Retrieved 2024-04-17, from [https://www.nature.com/](https://www.nature.com/articles/s43247-024-01324-8)
 533 [articles/s43247-024-01324-8](https://www.nature.com/articles/s43247-024-01324-8) (Publisher: Nature Publishing Group) doi:
 534 10.1038/s43247-024-01324-8
- 535 Hubanks, P., Platnick, S., King, M., & Ridgway, B. (2016). *MODIS Atmosphere*
 536 *L3 Gridded Product Algorithm Theoretical Basis Document (ATBD) & Users*
 537 *Guide* (Tech. Rep.). NASA EOS.
- 538 Ilyinskaya, E., Schmidt, A., Mather, T. A., Pope, F. D., Witham, C., Baxter, P.,
 539 ... Edmonds, M. (2017). Understanding the environmental impacts of large
 540 fissure eruptions: Aerosol and gas emissions from the 2014–2015 holuhraun
 541 eruption (iceland). *Earth and Planetary Science Letters*, 472, 309–322. Re-
 542 trieved from [https://www.sciencedirect.com/science/article/pii/](https://www.sciencedirect.com/science/article/pii/S0012821X17302911)
 543 [S0012821X17302911](https://www.sciencedirect.com/science/article/pii/S0012821X17302911) doi: <https://doi.org/10.1016/j.epsl.2017.05.025>
- 544 Ioannidis, E., Law, K. S., Raut, J.-C., Marelle, L., Onishi, T., Kirpes, R. M., ...
 545 Pratt, K. A. (2023). Modelling wintertime sea-spray aerosols under arctic
 546 haze conditions. *Atmospheric Chemistry and Physics*, 23(10), 5641–5678. Re-
 547 trieved from <https://acp.copernicus.org/articles/23/5641/2023/> doi:
 548 10.5194/acp-23-5641-2023
- 549 IPCC. (2023). The earth’s energy budget, climate feedbacks and climate sensitivity.
 550 In *Climate change 2021 – the physical science basis: Working group i contri-*
 551 *bution to the sixth assessment report of the intergovernmental panel on climate*
 552 *change* (p. 923–1054). Cambridge University Press.
- 553 Lana, A., Bell, T. G., Simó, R., Vallina, S. M., Ballabrera-Poy, J., Kettle, A. J., ...
 554 Liss, P. S. (2011). An updated climatology of surface dimethylsulfide concen-
 555 trations and emission fluxes in the global ocean. *Global Biogeochemical Cycles*,
 556 25(1). doi: 10.1029/2010GB003850
- 557 Lapere, R., Thomas, J. L., Marelle, L., Ekman, A. M. L., Frey, M. M., Lund,
 558 M. T., ... Zieger, P. (2023). The representation of sea salt aerosols
 559 and their role in polar climate within cmip6. *Journal of Geophysical Re-*
 560 *search: Atmospheres*, 128(6), e2022JD038235. Retrieved from [https://](https://agupubs.onlinelibrary.wiley.com/doi/abs/10.1029/2022JD038235)
 561 agupubs.onlinelibrary.wiley.com/doi/abs/10.1029/2022JD038235
 562 (e2022JD038235 2022JD038235) doi: <https://doi.org/10.1029/2022JD038235>
- 563 Li, G., Wieder, J., Pasquier, J. T., Henneberger, J., & Kanji, Z. A. (2022). Predict-
 564 ing atmospheric background number concentration of ice-nucleating particles
 565 in the arctic. *Atmospheric Chemistry and Physics*, 22(21), 14441–14454. Re-
 566 trieved from <https://acp.copernicus.org/articles/22/14441/2022/> doi:
 567 10.5194/acp-22-14441-2022
- 568 Lohmann, U., & Feichter, J. (2005, March). Global indirect aerosol effects: a re-
 569 view. *Atmospheric Chemistry and Physics*, 5(3), 715–737. Retrieved 2024-04-
 570 17, from <https://acp.copernicus.org/articles/5/715/2005/> (Publisher:
 571 Copernicus GmbH) doi: 10.5194/acp-5-715-2005
- 572 Lohmann, U., Feichter, J., Penner, J., & Leaitch, R. (2000). Indirect effect of sul-
 573 fate and carbonaceous aerosols: A mechanistic treatment. *Journal of Geophys-*
 574 *ical Research: Atmospheres*, 105(D10), 12193–12206. Retrieved from [https://](https://agupubs.onlinelibrary.wiley.com/doi/abs/10.1029/1999JD901199)
 575 agupubs.onlinelibrary.wiley.com/doi/abs/10.1029/1999JD901199 doi:
 576 <https://doi.org/10.1029/1999JD901199>
- 577 Lohmann, U., Lüönd, F., & Mahrt, F. (2016). *An Introduction to Clouds: From*
 578 *the Microscale to Climate*. Cambridge: Cambridge University Press. Re-
 579 trieved 2024-04-17, from [https://www.cambridge.org/core/books/](https://www.cambridge.org/core/books/an-introduction-to-clouds/F5A8096E7A3BD5C8FFD9208248DD1839)
 580 [an-introduction-to-clouds/F5A8096E7A3BD5C8FFD9208248DD1839](https://www.cambridge.org/core/books/an-introduction-to-clouds/F5A8096E7A3BD5C8FFD9208248DD1839) doi:
 581 10.1017/CBO9781139087513
- 582 Madeleine, J.-B., Hourdin, F., Grandpeix, J.-Y., Rio, C., Dufresne, J.-L., Vignon,
 583 E., ... Bonazzola, M. (2020). Improved representation of clouds in the
 584 atmospheric component lmdz6a of the ipsl-cm6a earth system model. *Jour-*

- 585 *nal of Advances in Modeling Earth Systems*, 12(10), e2020MS002046. Retrieved from <https://agupubs.onlinelibrary.wiley.com/doi/abs/10.1029/2020MS002046> (e2020MS002046 10.1029/2020MS002046) doi: <https://doi.org/10.1029/2020MS002046>
- 586
587
588
- 589 Malavelle, F. F., Haywood, J. M., Jones, A., Gettelman, A., Clarisse, L., Bauduin,
590 S., ... Thordarson, T. (2017, June). Strong constraints on aerosol–cloud in-
591 teractions from volcanic eruptions. *Nature*, 546(7659), 485–491. Retrieved
592 2024-04-17, from <https://www.nature.com/articles/nature22974> (Pub-
593 lisher: Nature Publishing Group) doi: 10.1038/nature22974
- 594 Marelle, L., Raut, J.-C., Law, K. S., Berg, L. K., Fast, J. D., Easter, R. C., ...
595 Thomas, J. L. (2017). Improvements to the wrf-chem 3.5.1 model for quasi-
596 hemispheric simulations of aerosols and ozone in the arctic. *Geoscientific Model*
597 *Development*, 10(10), 3661–3677. Retrieved from [https://gmd.copernicus](https://gmd.copernicus.org/articles/10/3661/2017/)
598 [.org/articles/10/3661/2017/](https://gmd.copernicus.org/articles/10/3661/2017/) doi: 10.5194/gmd-10-3661-2017
- 599 Müllenstädt, J., & Feingold, G. (2018, March). The Radiative Forcing of
600 Aerosol–Cloud Interactions in Liquid Clouds: Wrestling and Embracing
601 Uncertainty. *Current Climate Change Reports*, 4(1), 23–40. Retrieved
602 2024-04-18, from <https://doi.org/10.1007/s40641-018-0089-y> doi:
603 10.1007/s40641-018-0089-y
- 604 Nightingale, P. D., Malin, G., Law, C. S., Watson, A. J., Liss, P. S., Liddi-
605 coat, M. I., ... Upstill-Goddard, R. C. (2000). In situ evaluation of air-
606 sea gas exchange parameterizations using novel conservative and volatile
607 tracers. *Global Biogeochemical Cycles*, 14(1), 373–387. Retrieved from
608 <http://dx.doi.org/10.1029/1999GB900091> doi: 10.1029/1999GB900091
- 609 Pfeffer, M. A., Bergsson, B., Barsotti, S., Stefánsdóttir, G., Galle, B., Arellano, S.,
610 ... Mereu, L. (2018). Ground-based measurements of the 2014–2015 holuhraun
611 volcanic cloud (iceland). *Geosciences*, 8(1). Retrieved from [https://](https://www.mdpi.com/2076-3263/8/1/29)
612 www.mdpi.com/2076-3263/8/1/29 doi: 10.3390/geosciences8010029
- 613 Quaas, J., Arola, A., Cairns, B., Christensen, M., Deneke, H., Ekman, A. M. L., ...
614 Wendisch, M. (2020). Constraining the twomey effect from satellite observa-
615 tions: issues and perspectives. *Atmospheric Chemistry and Physics*, 20(23),
616 15079–15099. Retrieved 2024-04-17, from [https://acp.copernicus.org/](https://acp.copernicus.org/articles/20/15079/2020/)
617 [articles/20/15079/2020/](https://acp.copernicus.org/articles/20/15079/2020/) (Publisher: Copernicus GmbH) doi:
618 10.5194/acp-20-15079-2020
- 619 Quaas, J., Jia, H., Smith, C., Albright, A. L., Aas, W., Bellouin, N., ... Schulz, M.
620 (2022). Robust evidence for reversal of the trend in aerosol effective climate
621 forcing. *Atmospheric Chemistry and Physics*, 22(18), 12221–12239. Retrieved
622 from <https://acp.copernicus.org/articles/22/12221/2022/> doi:
623 10.5194/acp-22-12221-2022
- 624 Seinfeld, J. H., Bretherton, C., Carslaw, K. S., Coe, H., DeMott, P. J., Dunlea,
625 E. J., ... Wood, R. (2016). Improving our fundamental understanding
626 of the role of aerosol-cloud interactions in the climate system. *Proceed-*
627 *ings of the National Academy of Sciences*, 113(21), 5781–5790. Retrieved
628 from <https://www.pnas.org/doi/abs/10.1073/pnas.1514043113> doi:
629 10.1073/pnas.1514043113
- 630 Tegen, I., Hollrig, P., Chin, M., Fung, I., Jacob, D., & Penner, J. (1997). Con-
631 tribution of different aerosol species to the global aerosol extinction opti-
632 cal thickness: Estimates from model results. *Journal of Geophysical Re-*
633 *search: Atmospheres*, 102(D20), 23895–23915. Retrieved from [https://](https://agupubs.onlinelibrary.wiley.com/doi/abs/10.1029/97JD01864)
634 agupubs.onlinelibrary.wiley.com/doi/abs/10.1029/97JD01864 doi:
635 <https://doi.org/10.1029/97JD01864>
- 636 Thompson, G., & Eidhammer, T. (2014). A study of aerosol impacts on clouds
637 and precipitation development in a large winter cyclone. *Journal of the*
638 *Atmospheric Sciences*, 71(10), 3636 - 3658. Retrieved from [https://](https://journals.ametsoc.org/view/journals/atsc/71/10/jas-d-13-0305.1.xml)
639 journals.ametsoc.org/view/journals/atsc/71/10/jas-d-13-0305.1.xml

- doi: 10.1175/JAS-D-13-0305.1
- 640
641 Tilmes, S., Emmons, L., Buchholz, R., & Team, T. C. D. (2022). [data set]
642 *cesm2.2/cam-chem output for boundary conditions. ucar/ncar - atmospheric*
643 *chemistry observations and modeling laboratory*. (Accessed 01 FEB 2024) doi:
644 <https://doi.org/10.5065/XS0R-QE86>
- 645 Twomey, S. (1974, December). Pollution and the planetary albedo. *Atmospheric*
646 *Environment (1967)*, 8(12), 1251–1256. Retrieved 2024-03-19, from [https://](https://www.sciencedirect.com/science/article/pii/0004698174900043)
647 www.sciencedirect.com/science/article/pii/0004698174900043 doi: 10
648 .1016/0004-6981(74)90004-3
- 649 von Glasow, R., & Crutzen, P. J. (2004). Model study of multiphase dms oxidation
650 with a focus on halogens. *Atmospheric Chemistry and Physics*, 4(3), 589–608.
651 Retrieved from <https://acp.copernicus.org/articles/4/589/2004/> doi:
652 10.5194/acp-4-589-2004
- 653 von Salzen, K., Whaley, C. H., Anenberg, S. C., Van Dingenen, R., Klimont, Z.,
654 Flanner, M. G., ... Winter, B. (2022, October). Clean air policies are key
655 for successfully mitigating Arctic warming. *Communications Earth & Envi-*
656 *ronment*, 3(1), 1–11. Retrieved 2024-03-19, from [https://www.nature.com/](https://www.nature.com/articles/s43247-022-00555-x)
657 [articles/s43247-022-00555-x](https://www.nature.com/articles/s43247-022-00555-x) (Publisher: Nature Publishing Group) doi:
658 10.1038/s43247-022-00555-x
- 659 Wiedinmyer, C., Yokelson, R. J., & Gullett, B. K. (2014). Global Emissions of Trace
660 Gases, Particulate Matter, and Hazardous Air Pollutants from Open Burning
661 of Domestic Waste. *Environmental Science & Technology*, 48(16), 9523–9530.
662 doi: 10.1021/es502250z
- 663 Xu, K.-M., & Randall, D. A. (1996). A semiempirical cloudiness parameteriza-
664 tion for use in climate models. *Journal of Atmospheric Sciences*, 53(21), 3084
665 - 3102. Retrieved from [https://journals.ametsoc.org/view/journals/](https://journals.ametsoc.org/view/journals/atsc/53/21/1520-0469_1996_053_3084_ascpfu_2_0_co_2.xml)
666 [atsc/53/21/1520-0469_1996_053_3084_ascpfu_2_0_co_2.xml](https://journals.ametsoc.org/view/journals/atsc/53/21/1520-0469_1996_053_3084_ascpfu_2_0_co_2.xml) doi: 10.1175/
667 1520-0469(1996)053(3084:ASCPFU)2.0.CO;2
- 668 Zaveri, R. A., Easter, R. C., Fast, J. D., & Peters, L. K. (2008). Model for Simu-
669 lating Aerosol Interactions and Chemistry (MOSAIC). *Journal of Geophysical*
670 *Research: Atmospheres*, 113(D13). doi: 10.1029/2007JD008782
- 671 Zelinka, M. D., Smith, C. J., Qin, Y., & Taylor, K. E. (2023). Comparison of
672 methods to estimate aerosol effective radiative forcings in climate mod-
673 els. *Atmospheric Chemistry and Physics*, 23(15), 8879–8898. Retrieved
674 from <https://acp.copernicus.org/articles/23/8879/2023/> doi:
675 10.5194/acp-23-8879-2023

1 **Aerosol background concentrations influence**
2 **aerosol-cloud interactions as much as the choice of**
3 **aerosol-cloud parameterization**

4 **Louis Marelle¹, Gunnar Myhre², Jennie L. Thomas³, Jean-Christophe Raut¹**

5 ¹Sorbonne Université, UVSQ, CNRS, LATMOS, Paris, France

6 ²Center for International Climate Research, Oslo, Norway

7 ³Université Grenoble Alpes, CNRS, IRD, Grenoble INP, IGE, Grenoble, France

8 **Key Points:**

- 9 • 4 aerosol-cloud parameterizations tested in a regional model are consistent with
10 observed cloud changes during the 2014 Holuhraun eruption
11 • Liquid water path (LWP) observations during the eruption are not enough to ex-
12 clude large LWP adjustments in models
13 • Aerosol radiative impacts are as sensitive to background aerosols as to aerosol-cloud
14 interactions parameterization choice

Corresponding author: Louis Marelle, louis.marelle@latmos.ipsl.fr

Abstract

We use an independent observational estimate of aerosol-cloud interactions (ACI) during the 2014 Holuhraun volcanic eruption in Iceland to evaluate 4 ACI parameterizations in a regional model. All parameterizations reproduce the observed pattern of liquid cloud droplet size reduction during the eruption, but strongly differ on its magnitude and on the resulting effective radiative forcing (ERF). Our results contradict earlier findings that this eruption could be used to constrain liquid water path (LWP) adjustments in models, except to exclude extremely high LWP adjustments of more than 20 g m^{-2} . The modeled ERF is very sensitive to the non-volcanic background aerosol concentration: doubling the non-volcanic aerosol background weakens the ACI ERF by $\sim 30\%$. Since aerosol biases in climate models can be an order of magnitude or more, these results suggest that aerosol background concentrations could be a major and under-examined source of uncertainty for modeling ACI.

Plain Language Summary

Particles suspended in the atmosphere (aerosols) play a key role in cloud formation. These aerosol-cloud interactions have a major but uncertain influence on climate. We compare 4 different ways to calculate aerosol-cloud interactions in a numerical atmospheric model. We compare model results to observed changes in clouds measured from satellites during the Holuhraun eruption in Iceland in 2014, which released large amounts of volcanic gases forming atmospheric aerosols. We find that all 4 approaches reproduce the observed reduction in cloud droplet sizes during the eruption, but that they disagree on its intensity and its impacts on the Earth's energy budget. An earlier study found that aerosol-cloud interactions did not significantly increase the amount of liquid water in the clouds; using a more recent version of the satellite observations we find that large increases are possible. We also show that the eruption's impacts on the Earth's energy budget strongly depend on non-volcanic aerosols already present in the atmosphere: doubling non-volcanic aerosols reduces the impacts by $\sim 30\%$. Aerosol biases in climate models can be far greater, indicating that this could be a major source of uncertainty for aerosol-cloud interactions and for understanding past, present and future climates.

1 Introduction

In Earth's atmosphere, a liquid cloud droplet can only form on a preexisting aerosol serving as a cloud condensation nucleus (CCN). As a result, the abundance and properties of aerosols have a direct influence on the physical and optical properties of clouds, and ultimately on the radiative budget of the Earth, through a range of processes called aerosol-cloud interactions (ACI, e.g. Lohmann & Feichter, 2005). The effective radiative forcing of ACI is currently estimated at -0.8 W m^{-2} , with likely values ranging from -1.45 to -0.25 W m^{-2} (IPCC, 2023). Despite the importance of ACI forcing for climate, this very wide uncertainty range has not been reduced significantly in recent years, and ACI remain the main source of uncertainty for quantifying anthropogenic radiative forcing, and a key physical uncertainty in climate projections.

Aerosols have a cooling effect on the global climate, but clean air policies have helped reduce aerosol pollution in recent years. There is evidence that improvements in air quality have also reduced aerosol cooling globally, revealing more of the underlying greenhouse gas warming trend (Quaas et al., 2022; Hodnebrog et al., 2024). In the Arctic, a region particularly sensitive to climate change, this "unmasking" of greenhouse warming may have been responsible for $+0.8^\circ\text{C}$ of additional warming from 1990 to 2015, half of the anthropogenic warming trend during the same period (von Salzen et al., 2022). These trends will likely continue in the future because of further emission reductions. In order to improve climate projections and to understand past changes, and to inform the policies that consider the trade-offs between short term and long term climate strate-

gies, it is thus critical to better constrain the ACI forcing and the main causes of uncertainty between models.

The impacts of ACI are hard to constrain in models because of the complexity of the processes involved, from the underlying microphysical changes to the interactions with cloud-scale and large-scale dynamics (e.g., Lohmann et al., 2016). To the first order, increasing aerosol concentrations increases liquid cloud droplet numbers and reduces cloud droplet size, forming optically thicker clouds than in aerosol-poor conditions (Twomey, 1974). In order to represent this process, climate models use ACI parameterizations of varying complexities, but it is unclear how much this range of parameterizations influences the predicted ACI radiative forcing uncertainty (Ekman, 2014), or how to best evaluate them against observations.

In fact, modeled ACI are also difficult to evaluate because the effects of ACI are very hard to observe directly. It is possible to compare observations of polluted clouds from unpolluted clouds, but attributing the differences to ACI requires very large datasets for controlling for all other causes of variability. Satellites could provide such a dataset, but they have limited sensitivity to cloud microphysics and are not currently able to estimate vertically resolved aerosol concentrations inside clouds (Quaas et al., 2020). Furthermore, due to the magnitude of anthropogenic and natural emissions of aerosols and their precursors, it is not feasible either to conduct controlled field experiments, such as emitting large enough amounts of aerosols during a long enough period. Large volcanic eruptions can be thought of as rare natural opportunistic experiments that can help us circumvent this problem (Christensen et al., 2022).

The Holuhraun fissure eruption in Iceland, from late August 2014 to February 2015, emitted the equivalent of 2 years of the European Union’s anthropogenic SO_2 emissions in just 6 months (Pfeffer et al., 2018; EEA, 2014), with most of the emissions occurring during the first two months of the eruption. During this time, observed cloud droplet sizes in the North Atlantic were reduced far outside the range of natural variability, due to ACI from volcanic aerosols. This independent observational estimate of ACI was compared previously to the predictions of climate models, showing that several models were inconsistent with observations (Malavelle et al., 2017).

In this study, we compare observed ACI in liquid clouds during the Holuhraun eruption against the predictions of 4 different ACI parameterizations in the same model framework. Specifically, we evaluate how well the different ACI parameterizations reproduce observed liquid cloud changes during the 2014 Holuhraun eruption, we quantify the uncertainty range in ACI radiative effect resulting from the choice of parameterization, and we compare this parameterization uncertainty to the uncertainty due to aerosol biases in the model. We show that the background aerosol concentration is a critical factor for modeling ACI accurately, and we discuss the wider implications for radiative forcing and climate modeling in the conclusion.

2 Methods

2.1 WRF-Chem 4.3.3 model

We perform simulations with the Weather Research and Forecasting model including chemistry (WRF-Chem, Grell et al., 2005), starting on 2014-08-15 and ending on 2014-11-01, allowing for 2 weeks of initial spin-up before the start of the eruption on 2014-08-29. The simulation domain is approximately $6000 \text{ km} \times 6000 \text{ km}$ in size, and centered on Iceland. The horizontal resolution is $50 \text{ km} \times 50 \text{ km}$ with 72 vertical levels between the surface and 50 hPa.

112 All simulations are performed with WRF-Chem version 4.3.3, including optimiza-
 113 tions for polar regions described in Marelle et al. (2017). New model updates since Marelle
 114 et al. (2017) are described below, including ACI developments presented in Section 2.1.4.

115 **2.1.1 WRF-Chem chemistry-aerosol setup**

116 Within WRF-Chem, we use the MOZART gas-phase chemistry mechanism (Emmons
 117 et al., 2010), and the MOSAIC-4bin sectional aerosol model (Zaveri et al., 2008) includ-
 118 ing aqueous chemistry (a setup called MOZART-MOSAIC-4BIN-AQ in WRF-Chem).
 119 Initial and time-varying boundary conditions for trace gases and aerosols are from the
 120 CAM-Chem model (Tilmes et al., 2022). For this study, we also update the dimethyl-
 121 sulfide (DMS) chemistry scheme in MOZART-MOSAIC-4bin-AQ to von Glasow and Crutzen
 122 (2004). The updated DMS mechanism includes MSA aerosols and the associated het-
 123 erogeneous chemistry. It was partly implemented in WRF-Chem for the CBM-Z and CRIMECH
 124 mechanisms by Archer-Nicholls et al. (2014); we include it fully in MOZART-MOSAIC-
 125 4BIN-AQ.

126 **2.1.2 WRF-Chem meteorological setup**

127 In our simulations, grid-scale cloud microphysics are modeled by the 2-moment Thomp-
 128 son Aerosol-Aware scheme (Thompson & Eidhammer, 2014), and subgrid clouds by the
 129 Grell-3 cumulus scheme (Grell & Dévényi, 2002). We modified the cloud fraction diag-
 130 nosis in WRF-Chem to follow Xu and Randall (1996). Initial and time-varying (6 hours)
 131 boundary conditions for meteorology are taken from the ERA5 reanalysis (Copernicus
 132 Climate Change Service, 2017), and spectral nudging to ERA5 is also applied for wind
 133 and temperature features over the 700 km scale. The full meteorological setup is pro-
 134 vided in Table S1.

135 **2.1.3 Emissions used in WRF-Chem simulations**

136 Daily varying volcanic SO₂ emissions and plume emission heights for the Holuhraun
 137 eruption are from Pfeffer et al. (2018). Emissions are injected in WRF-Chem as a uni-
 138 form source from the provided plume bottom altitude to plume top, at the location of
 139 the eruption (64.87°N, 16.84°W). 1% of SO₂ emissions are emitted as primary sulfate (Ilyinskaya
 140 et al., 2017).

141 Anthropogenic emissions are from the CAMSv4.2 inventory, applying sector-dependent
 142 daily and hourly emission variations and vertical profiles (Denier van der Gon et al., 2011;
 143 Archer-Nicholls et al., 2014). 3% of anthropogenic SO_x is emitted as primary sulfate (Alexander
 144 et al., 2009). Open biomass burning emissions are from FINNv1.5 (Wiedinmyer et al.,
 145 2014).

146 Natural sea spray emissions from open oceans follow Ioannidis et al. (2023) but do
 147 not include experimental emissions of marine organics. Dust emissions are included (Chin
 148 et al., 2002), but are very low in the domain. Terrestrial biogenic emissions are from MEGANv2.1
 149 (Guenther et al., 2012), and DMS emissions use the ocean climatology of Lana et al. (2011)
 150 with the sea-air flux from Nightingale et al. (2000).

151 **2.1.4 Aerosol-cloud parameterizations implemented and compared in WRF- 152 Chem**

153 We compare 4 aerosol-cloud interaction parameterizations in the WRF-Chem model:

- 154 • TE14: The ACI parameterization of the Thompson aerosol-aware cloud model (Thompson
 155 & Eidhammer, 2014) calculates cloud droplet formation based on the thermody-
 156 namical conditions in the clouds and 2 aerosol parameters, the water-friendly and

ice-friendly aerosol number concentrations. In the base version of the model, TE14 initializes these aerosol numbers from a fixed climatology. Here, TE14 uses aerosol numbers predicted by WRF-Chem. The water-friendly aerosol is set as the hydrophilic volume fraction (sulfate, nitrate, ammonium, sea salt, MSA) of the total WRF-Chem aerosol number in each size bin. To eliminate a source of variability between simulations, ice-friendly aerosol numbers are set to the fixed minimum model value of 5 L^{-1} . This is consistent with the negligible emission of ice-active volcanic dust in the eruption, and with the low ice nucleating particle numbers at high latitudes (Li et al., 2022).

- ARG02: The parameterization of Abdul-Razzak and Ghan (2002) calculates aerosol activation and cloud droplet numbers based on aerosol size, number, and hygroscopicity in each size bin. It was already included in the WRF-Chem chemistry code as part of the Morrison and Lin microphysics schemes. We reimplemented ARG02 into Thompson microphysics, consistently with TE14. For consistency, both TE14 and ARG02 include the same sub-grid distribution of updraft velocity from Ghan et al. (1997).
- BL95: The parameterization of Boucher and Lohmann (1995) predicts cloud droplet number concentrations as a function of accumulation-mode sulfate mass. We include it in WRF-Chem by overwriting the cloud droplet number passed by Thompson microphysics to the radiation code by the BL95-predicted value.
- LMDZ6: This parameterization, based on BL95, is used in the LMDZ6 climate model (Madeleine et al., 2020), and predicts cloud droplet number concentrations as a function of accumulation-mode soluble mass. The implementation is the same as in BL95, using the WRF-Chem mass of sulfate, ammonium, and sea salt. The LMDZ6 model does not include nitrate or MSA, so these were not used for the calculation.

By design, LMDZ6 and BL95 only represent the effect of aerosols on cloud droplet number and radiation, the so-called “first indirect effect” (Twomey, 1974), while ARG02 and TE14 are also able to represent microphysical adjustments of clouds to ACI, influencing precipitation, cloud dynamics and lifetime, and liquid water path, the “second indirect effect” (Albrecht, 1989).

For each of these 4 ACI parameterizations, we perform a control simulation (VOLC) that includes volcanic emissions, and a counterfactual simulation (noVOLC) without volcanic emissions, for a total of 8 simulations. The difference VOLC-noVOLC is used to estimate the effect of ACI due to volcanic aerosols. In order to further reduce differences between simulations, only the ARG02 simulation is run as a fully coupled WRF-Chem simulation with prognostic aerosols. TE14, LMDZ6 and BL95 aerosols are instead forced by the 3-hourly aerosol fields produced by ARG02. Furthermore, to remove the contribution of direct aerosol-radiation interactions (ARI) from the VOLC-noVOLC signal, all 8 simulations include simplified ARI from identical climatological aerosol fields (Tegen et al., 1997), instead of using prognostic WRF-Chem aerosols. This workflow also has the advantage of speeding up the calculations significantly, allowing for the sensitivity simulations presented in Section 3.4. But the main advantage is that all 4 ACI setups use the exact same meteorological setup, ARI, ice nucleation scheme, and aerosol fields for liquid cloud ACI, ensuring that the only difference between them is the choice of the liquid-cloud ACI parameterization.

2.2 MODIS observations of clouds for evaluating modeled ACI

We estimate the effect of the eruption on cloud properties using observations from the MODIS instruments on board of the Aqua and Terra satellites, using the $1^\circ \times 1^\circ$ monthly gridded cloud products MYD08_M3.6.1 and MOD08_M3.6.1. Specifically, we compute

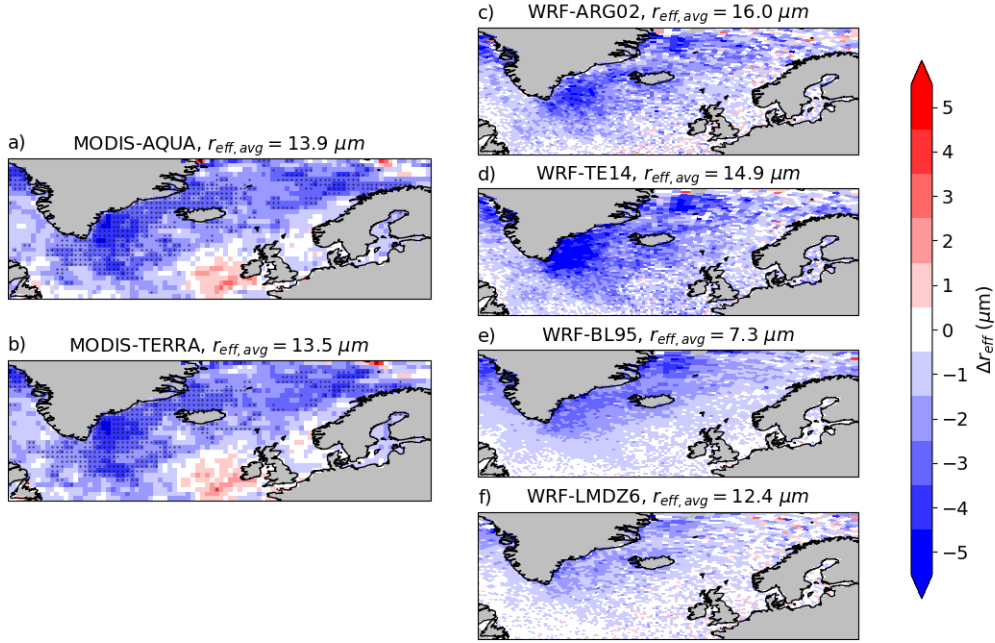


Figure 1. Cloud liquid droplet effective radius response to volcanic aerosols. a) MODIS-AQUA and b) MODIS-Terra liquid cloud droplet effective radius anomaly in October 2014, 2002-2022 baseline. c-d-e-f) WRF-Chem liquid cloud droplet effective radius anomaly due to volcanic emissions (VOLC - noVOLC anomaly, October 2014 average) using the c) ARG02 d) TE14 e) BL95 and f) LMDZ6 ACI parameterizations. Above each panel, $r_{eff,avg}$ gives the regionally averaged r_{eff} in October 2014, observed or modeled in the Volc simulation.

207 the October 2014 MODIS liquid effective radius (r_{eff}) and liquid water path (LWP) anomalies from the October 2002-2022 climatological baseline (excluding 2014).
 208

209 For a like-for-like comparison of MODIS and WRF-Chem, WRF-Chem r_{eff} and
 210 LWP are postprocessed to follow the MODIS monthly L3 product procedure (Hubanks
 211 et al., 2016). Cloud properties are extracted from the 3-hourly WRF-Chem output, keep-
 212 ing only daytime scenes with solar zenith angles less than 81.373° , producing daily maps,
 213 which are then aggregated to monthly gridded maps of r_{eff} and LWP. MODIS in-cloud
 214 LWP is compared with WRF-Chem’s grid-scale LWP by multiplying the in-cloud val-
 215 ues with the liquid cloud fraction. Regionally averaged comparisons in Section 3 are taken
 216 over ocean points only, from latitudes 47°N to 77°N , longitudes 60°W to 30°E , with area-
 217 weighted averaging.

218 3 Results

219 3.1 Effect of the eruption on the cloud droplet radius, and sensitivity 220 to ACI parameterization

221 In October 2014, during the Holuhraun eruption, the MODIS cloud r_{eff} was sig-
 222 nificantly smaller than usual. On average in the North Atlantic, the effective radius anomaly
 223 $\Delta r_{eff} = -1.48\mu\text{m}$ (Figure 1), outside 2 standard deviations of the climatology ($2\sigma =$
 224 $1.14\mu\text{m}$). This is a consequence of ACI from the additional volcanic aerosols (Malavelle
 225 et al., 2017).

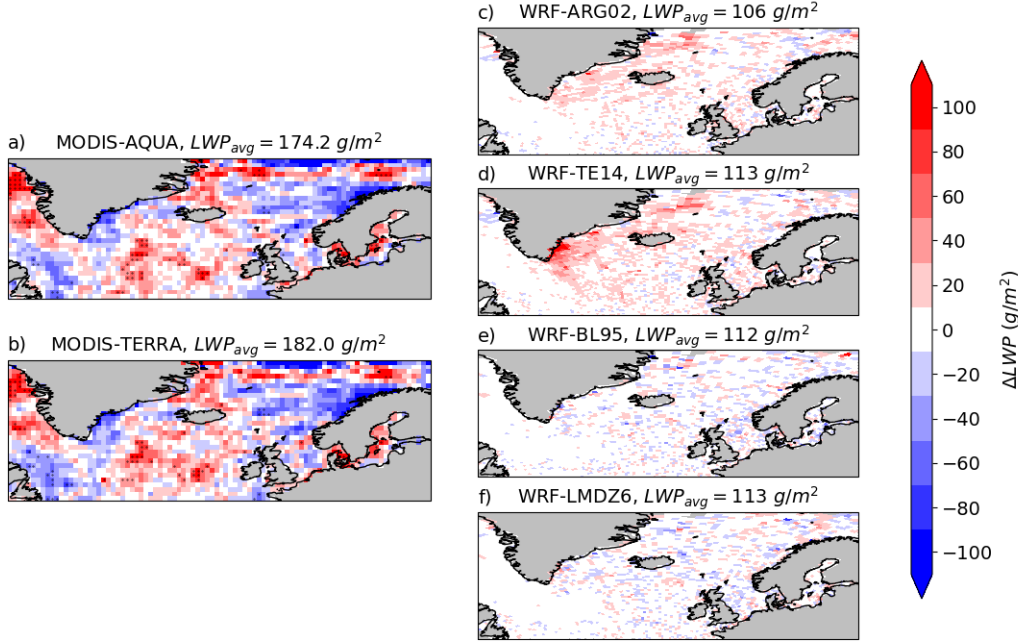


Figure 2. Liquid water path response to volcanic aerosols. a) MODIS-AQUA and b) MODIS-Terra liquid water path radius anomaly observed in October 2014, 2002-2022 baseline. c-d-e-f) WRF-Chem liquid water path anomaly due to volcanic emissions (VOLC - NOVOLC anomaly), October 2014 average, using the b) ARG02 c) TE14 d) BL95 and e) LMDZ6 ACI parameterizations. BL95 and LMDZ6 do not include the second indirect effect.

226 The 4 ACI parameterizations predict a strong r_{eff} reduction in the domain, and
 227 reproduce the overall geographical pattern of this change. The modeled Δr_{eff} is sensi-
 228 tive to the choice of ACI parameterization, with $-1.20 \mu m$, $-1.63 \mu m$, $-1.09 \mu m$ and $-$
 229 $0.66 \mu m$ for ARG02, TE14, BL95, and LMDZ6 respectively (Table S2). The simple BL95
 230 parameterization predicts a reasonable Δr_{eff} anomaly, but strongly underestimates the
 231 observed absolute r_{eff} by -47% . Conversely, LMDZ6 reproduces the observed r_{eff} but
 232 strongly underestimates the observed Δr_{eff} by -55% . Implications for radiative forcing
 233 in LMDZ6 are discussed in Section 3.3.

234 3 of the 4 parameterizations underestimate Δr_{eff} . This could be a limitation of
 235 the ACI parameterizations themselves, or it could be due to underestimated aerosols in
 236 the volcanic plume. During the eruption, the WRF-ARG02 simulation reproduces the
 237 observations of fine particle mass concentration ($PM_{2.5}$) at European surface sites very
 238 well (Figure S1a). Before the start of the eruption, background aerosol sulfate is also well
 239 represented, but after the eruption begins in late August, the model underestimates sul-
 240 fate at surface sites (Figure S1b). To our knowledge, the vertical distribution of aerosols
 241 in the Holuhraun plume was not observed, so it is not clear if the same bias is present
 242 at higher altitudes where aerosols interact with clouds, or if it could be due to errors in
 243 the downward mixing of the volcanic plume into the boundary layer. In the following,
 244 we will focus on the sensitivity of ACI to parameterizations and aerosols in the model.

3.2 Effect of the eruption on the liquid water path, and sensitivity to ACI parameterization

Figure 2 compares the observed and modeled LWP anomaly due to the eruption in October 2014. WRF-ARG02 and WRF-TE14 show a weak regionally-averaged ΔLWP response of $+3.9 \text{ g m}^{-2}$ and $+6.8 \text{ g m}^{-2}$ respectively (Table S2), well below the threshold of observed natural variability ($2\sigma = 19.3 \text{ g m}^{-2}$). It is important to note that BL95 and LMDZ6 do not include cloud microphysical adjustments to the r_{eff} change (the second indirect effect). For BL95 and LMDZ6, LWP changes are then only due to random variability and small dynamical adjustments to the first indirect effect, and are as expected close to zero. The absolute regionally-averaged LWP is close to 110 g m^{-2} with all parameterizations, significantly lower than MODIS observations ($\sim 180 \text{ g m}^{-2}$), but higher than the climate model simulations in Malavelle et al. (2017) (mean LWP $\sim 60 \text{ g m}^{-2}$).

Using MODIS products from version 5.1, Malavelle et al. (2017) found that the impact of the eruption on LWP was very limited, and could not exceed 9 g m^{-2} . They concluded that large LWP adjustments in climate models were inconsistent with these observations. Using revised LWP from MODIS version 6.1, and a longer climatological period (2002-2022 excluding 2014 instead of 2002-2013) we find a much larger significance threshold $2\sigma = 19.3 \text{ g m}^{-2}$, which is consistent with even the largest climate model ΔLWP of 16.3 g m^{-2} from Malavelle et al. (2017).

A recent study suggested that the cloud response to the Holuhraun eruption could be dominated by cloud fraction adjustment, instead of changes in LWP or r_{eff} (Chen et al., 2022). This is not the case here, and WRF-ARG02 and WRF-TE14 predict positive but very small cloud fraction adjustments of $+0.4$ and $+0.8$ percentage points respectively (Figure S2 and Table S2).

3.3 Sensitivity of the aerosol radiative impact to the ACI parameterization

The regionally averaged radiative effect of ACI on the net shortwave flux at top-of-atmosphere (ERF_{aci}^{SW}) in October 2014 is -1.12 , -1.97 , -1.08 and -0.34 W m^{-2} for ARG02, TE14, BL95, and LMDZ6 respectively (Table S2). The weak -0.34 W m^{-2} ERF_{aci}^{SW} in LMDZ6 is consistent with its low Δr_{eff} response. This could explain why the IPSL-CM6 climate model, where LMDZ6 is hosted, has the weakest ACI effective radiative forcing among CMIP6 models (Zelinka et al., 2023). Despite very different approaches and complexities, ARG02 and BL95 predict a similar ERF_{aci}^{SW} . TE14, which best reproduces the observed r_{eff} and Δr_{eff} , also predicts the strongest forcing, nearly 2 times stronger than ARG02 and BL95.

3.4 Sensitivity of the modeled cloud response to the aerosol background

Aerosol-cloud interactions are strongly non-linear. For this reason, the modeled radiative impact of an aerosol perturbation is sensitive to the absolute aerosol concentrations in the background state (Carslaw et al., 2013; Lohmann et al., 2000). In order to estimate the sensitivity of the modeled ACI to the non-volcanic aerosol background, we perform sensitivity experiments in the WRF-Chem model by perturbing the non-volcanic aerosol climatology aer (units $\mu\text{g kg}^{-1}$ and kg^{-1}) used to force the TE14, LMDZ6, and BL95 parameterizations by a factor $\alpha = 0.5, 0.75, 1.5, \text{ or } 2$.

$$aer_{NoVolc,perturbed} = \alpha \times aer_{NoVolc} \quad (1)$$

$$aer_{Volc,perturbed} = \alpha \times aer_{NoVolc} + (aer_{Volc} - aer_{NoVolc}) \quad (2)$$

For each sensitivity simulation, we calculate the VOLC-noVOLC Δr_{eff} and ERF_{aci}^{SW} and compare it to the value from the unperturbed reference run, as a function of the perturbation anomaly $\alpha - 1.0$, which is equal to zero for the unperturbed case. Aerosols

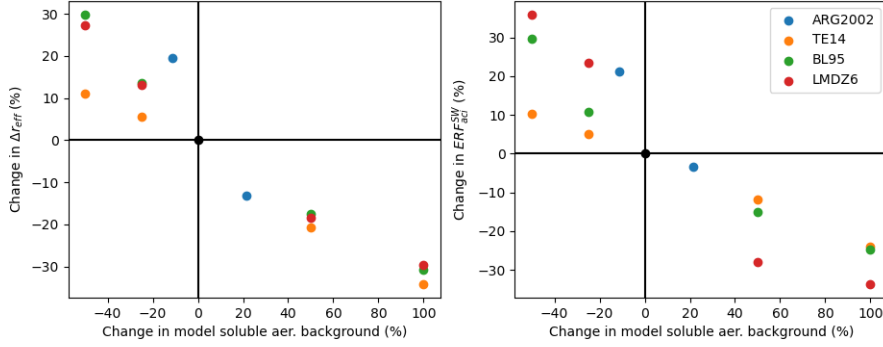


Figure 3. Sensitivity of volcanic aerosol-cloud-interactions to the non-volcanic aerosol background concentration. (left) effective radius anomaly during the eruption (right) indirect short-wave radiative effect of the eruption at top-of-atmosphere. All values are given as percentage changes from the unperturbed reference simulations.

cannot be perturbed directly in ARG02, because they are not forced but computed prognostically in the model. In order to estimate the sensitivity of ARG02 to background aerosol concentrations, we perturb instead the marine emissions of sea spray and DMS. Since these sensitivity simulations are fully coupled, they are computationally costly, and we only perform 2 sensitivity simulations with emissions multiplied by 0.5 and 2.

Figure 3 shows that the droplet effective radius and the aerosol forcing are very sensitive to the non-volcanic aerosol background. When the background aerosol concentration is doubled (+100%), the Δr_{eff} is ~ 30 to 35% weaker than in the reference run, and the ERF_{aci}^{SW} is ~ 25 to 35% weaker, even though the volcanic aerosol perturbation is exactly the same. When the background is divided by 2 (-50%), the Δr_{eff} is ~ 10 to 30% stronger than in the reference run, and the ERF_{aci}^{SW} is ~ 10 to 40% larger. Since local biases in aerosol background concentrations can often be an order of magnitude or more in climate models (e.g. Lapere et al., 2023; Bian et al., 2024), this effect could be a major source of uncertainty for radiative forcing calculations.

4 Discussion, conclusions, and recommendations for climate modeling

In this study, we compare 4 ACI parameterizations in the same regional modeling framework during a large volcanic eruption. We calculate the sensitivity of the cloud response and the aerosol radiative forcing to the choice of parameterization, and the sensitivity of volcanic ACI to the non-volcanic aerosol background.

All 4 ACI parameterizations reproduce the pattern and overall magnitude of the observed change in liquid cloud droplet effective radius during the eruption, but LMDZ6 underestimates this change. Modeled ACI are sensitive to ACI parameterization in terms of effective radius and radiative impacts. The ACI radiative impact is very weak for the LMDZ6 ACI parameterization, and we believe that this choice of parameterization could explain the low aerosol ERF in the associated IPSL-CM6 climate model. We did not test the full parameterization panel from CMIP6 models, and our results certainly underestimate the full range of sensitivity to ACI parameterization; however, the types of parameterizations tested are representative of this generation of climate models.

321 Our study disagrees with one of the main conclusions of Malavelle et al. (2017):
322 we find that this volcanic case study cannot be used to constrain the ACI LWP adjust-
323 ment in climate models, except to rule out very high regional LWP changes of more than
324 $\sim 20 \text{ g m}^{-2}$. These values are much larger than the magnitude of the LWP change due
325 to ACI in WRF-Chem in either ARG02 or TE14 ($\sim 5 \text{ g m}^{-2}$), and consistent with even
326 the largest LWP changes predicted by climate models in Malavelle et al. (2017). Our sim-
327 ulations and those of Malavelle et al. (2017) underestimate the observed LWP in the re-
328 gion, so further work is needed to fully understand LWP adjustments in models.

329 We find that the modeled cloud response to the eruption is also very sensitive to
330 the non-volcanic background aerosol concentration: a doubling of the aerosol background
331 translates into a $\sim -30\%$ change in ACI radiative forcing. This sensitivity is worrying
332 because biases in aerosol mixing ratio in climate models can be far greater. Allen and
333 Landuyt (2014) found that model spread for black carbon aerosols in CMIP5 is up to
334 2 orders of magnitude in the free troposphere, and Lapere et al. (2023); Bian et al. (2024)
335 showed that aerosol differences between models in the remote marine and polar tropo-
336 sphere, respectively, can be 1 or 2 orders of magnitude.

337 Nearly 25 years ago, Lohmann et al. (2000) showed that aerosol-cloud radiative forc-
338 ing in the ECHAM4 climate model was sensitive to the pre-industrial aerosol burden.
339 Based on this result, Lohmann and Feichter (2005) suggested that the large differences
340 in ERF_{ACI} between models could be due to “the dependence of the indirect aerosol ef-
341 fect on the background aerosol concentration”. Carslaw et al. (2013) later found that
342 uncertainties in natural emissions could account for 45% of the ERF_{ACI} uncertainty in
343 a single global model. However, to our knowledge, the precise contribution of these er-
344 rors to the large CMIP multimodel RF_{ACI} uncertainty has not been investigated since,
345 and was not identified as a major issue in recent efforts for understanding aerosol ERF
346 (Fiedler et al., 2023; Bellouin et al., 2020; Quaas et al., 2020; Mülmenstädt & Feingold,
347 2018; Seinfeld et al., 2016). In light of our results and of earlier literature, we recommend
348 a systematic analysis of how the natural aerosol background influences the ERF_{ACI} spread
349 in climate models. If background aerosols are indeed important, improving the repre-
350 sentation of natural aerosols such as sea-spray, sulfate from oceanic DMS, and biomass
351 burning could be a more efficient pathway for reducing ACI uncertainties than difficult
352 improvements in complex aerosol-cloud processes.

353 For this purpose, a detailed evaluation of aerosols in climate models is critical. ACI
354 are determined by aerosol properties within clouds, and are especially sensitive to aerosol
355 concentrations and aerosol size (Dusek et al., 2006). However, aerosols in climate mod-
356 els are usually evaluated in terms of vertically integrated bulk properties such as Aerosol
357 Optical Depth (AOD), which is also the usual CCN proxy for observational estimates
358 of the aerosol ERF (Bellouin et al., 2020; Gryspeerdt et al., 2023). This is concerning,
359 because large errors in aerosol concentrations, vertical distributions, water uptake, and
360 size distributions can compensate to give a reasonable AOD in models (Quaas et al., 2020).
361 In this context, we also recommend routine evaluations and comparisons of aerosol ver-
362 tical distributions in climate models, for example using the now extensive LiDAR and
363 aircraft measurement datasets.

364 The sensitivity of ACI to aerosol background is not just important in the pre-industrial
365 period and for quantifying ERF_{ACI} in climate models, which has been the focus until
366 now. Our results suggest that tackling these issues and improving the representation of
367 background aerosols in models could also help us better understand the effect of ACI at
368 shorter time scales, including the influence of ACI on specific extreme events, its effect
369 on meteorological forecasts, and the effect of recent and future clean air policies on cli-
370 mate.

Open Research Section

The updated WRF-Chem 4.3.3 model version used in this study can be found at <https://doi.org/10.5281/zenodo.12544534>. The WRF preprocessing system (WPS) is available at <https://archive.softwareheritage.org/swh:1:dir:21227ff84043afa53bb870245da4061fe7f0c7ab;origin=https://github.com/wrf-model/WPS;visit=swh:1:snp:096256316e752343901abad92a7dd9c2529f48cb;anchor=swh:1:rev:5a2ae63988e632405a4504cfb143ce7f0230a7a0>. WRF-Chem preprocessor tools (mozbc, fire_emiss and bio_emiss) are available at <https://www2.acom.ucar.edu/wrf-chem/wrf-chem-tools-community>. WRF-Chem run and setup scripts, preprocessing codes, and post-processing codes created for this study can be found at <https://doi.org/10.5281/zenodo.12544354>.

ERA5 input data on pressure and surface levels for WRF can be obtained at <https://doi.org/10.24381/cds.143582cf>. CAM-Chem input data for initial and boundary conditions is available at <https://doi.org/10.5065/NMP7-EP60..> CAMSv4.2 emissions are available at <https://ads.atmosphere.copernicus.eu/cdsapp#!/dataset/cams-global-emission-inventories> FINNv1.5 emissions are distributed at <https://www.acom.ucar.edu/Data/fire/>. The Lana DMS climatology can be found at https://www.bodc.ac.uk/solas_integration/implementation_products/group1/dms/documents/dmsclimatology.zip.

MODIS satellite observations from the MYD08_M3_6_1 and MOD08_M3_6_1 products can be retrieved from https://doi.org/10.5067/MODIS/MYD08_M3_061 and https://doi.org/10.5067/MODIS/MOD08_M3_061. Observations of atmospheric composition used in the supplement are from <https://ebas.nilu.no/>.

Acknowledgments

This project has received funding from Horizon Europe programme under Grant Agreement No 101137680 via project CERTAINTY (Cloud-aERosol inTeractions & their impActs IN The earth sYstem); from the European Union's Horizon 2020 research and innovation programme under Grant agreement No 101003826 via project CRiceS (Climate Relevant interactions and feedbacks: the key role of sea ice and Snow in the polar and global climate system); and from the project SUPER (no. 250573) funded through the Research Council of Norway. This research has been partly funded by French National Research Agency (ANR) via the project MPC2 (n° ANR-22-CEA01-0009-02). Computer analyses benefited from access to IDRIS HPC resources (GENCI allocations A011017141 and A013017141), and from the IPSL mesocenter ESPRI facility which is supported by CNRS, UPMC, Labex L-IPSL, CNES and Ecole Polytechnique. We acknowledge use of the WRF-Chem preprocessor tools mozbc, fire_emiss and bio_emiss provided by the Atmospheric Chemistry Observations and Modeling Lab (ACOM) of NCAR. We acknowledge ECCAD for the archiving and distribution of the CAMS emissions data.

References

- Abdul-Razzak, H., & Ghan, S. J. (2002). A parameterization of aerosol activation 3. sectional representation. *Journal of Geophysical Research: Atmospheres*, 107(D3), AAC 1-1-AAC 1-6. Retrieved from <https://agupubs.onlinelibrary.wiley.com/doi/abs/10.1029/2001JD000483> doi: <https://doi.org/10.1029/2001JD000483>
- Albrecht, B. A. (1989, September). Aerosols, Cloud Microphysics, and Fractional Cloudiness. *Science*, 245(4923), 1227–1230. Retrieved 2024-03-19, from <https://www.science.org/doi/10.1126/science.245.4923.1227> (Publisher: American Association for the Advancement of Science) doi: [10.1126/science.245.4923.1227](https://doi.org/10.1126/science.245.4923.1227)

- 420 Alexander, B., Park, R. J., Jacob, D. J., & Gong, S. (2009). Transition metal-
 421 catalyzed oxidation of atmospheric sulfur: Global implications for the sulfur
 422 budget. *Journal of Geophysical Research: Atmospheres*, *114*(D2). Retrieved
 423 from [https://agupubs.onlinelibrary.wiley.com/doi/abs/10.1029/](https://agupubs.onlinelibrary.wiley.com/doi/abs/10.1029/2008JD010486)
 424 [2008JD010486](https://doi.org/10.1029/2008JD010486) doi: <https://doi.org/10.1029/2008JD010486>
- 425 Allen, R. J., & Landuyt, W. (2014). The vertical distribution of black carbon in
 426 cmip5 models: Comparison to observations and the importance of convective
 427 transport. *Journal of Geophysical Research: Atmospheres*, *119*(8), 4808–4835.
 428 Retrieved from [https://agupubs.onlinelibrary.wiley.com/doi/abs/](https://agupubs.onlinelibrary.wiley.com/doi/abs/10.1002/2014JD021595)
 429 [10.1002/2014JD021595](https://doi.org/10.1002/2014JD021595) doi: <https://doi.org/10.1002/2014JD021595>
- 430 Archer-Nicholls, S., Lowe, D., Utembe, S., Allan, J., Zaveri, R. A., Fast, J. D.,
 431 ... McFiggans, G. (2014). Gaseous chemistry and aerosol mecha-
 432 nism developments for version 3.5.1 of the online regional model, wrf-
 433 chem. *Geoscientific Model Development*, *7*(6), 2557–2579. Retrieved
 434 from <https://gmd.copernicus.org/articles/7/2557/2014/> doi:
 435 [10.5194/gmd-7-2557-2014](https://doi.org/10.5194/gmd-7-2557-2014)
- 436 Bellouin, N., Quaas, J., Gryspeerdt, E., Kinne, S., Stier, P., Watson-Parris, D.,
 437 ... Stevens, B. (2020). Bounding global aerosol radiative forcing of
 438 climate change. *Reviews of Geophysics*, *58*(1), e2019RG000660. Re-
 439 trieved from [https://agupubs.onlinelibrary.wiley.com/doi/abs/](https://agupubs.onlinelibrary.wiley.com/doi/abs/10.1029/2019RG000660)
 440 [10.1029/2019RG000660](https://doi.org/10.1029/2019RG000660) (e2019RG000660 10.1029/2019RG000660) doi:
 441 <https://doi.org/10.1029/2019RG000660>
- 442 Bian, H., Chin, M., Colarco, P. R., Apel, E. C., Blake, D. R., Froyd, K., ... Zhu,
 443 J. (2024). Observationally constrained analysis of sulfur cycle in the ma-
 444 rine atmosphere with nasa atom measurements and aerocom model simula-
 445 tions. *Atmospheric Chemistry and Physics*, *24*(3), 1717–1741. Retrieved
 446 from <https://acp.copernicus.org/articles/24/1717/2024/> doi:
 447 [10.5194/acp-24-1717-2024](https://doi.org/10.5194/acp-24-1717-2024)
- 448 Boucher, O., & Lohmann, U. (1995, Jan). The sulfate-ccn-cloud albedo effect: A
 449 sensitivity study with two general circulation models. *Tellus B: Chemical and*
 450 *Physical Meteorology*. doi: [10.3402/tellusb.v47i3.16048](https://doi.org/10.3402/tellusb.v47i3.16048)
- 451 Carslaw, K. S., Lee, L. A., Reddington, C. L., Pringle, K. J., Rap, A., Forster,
 452 P. M., ... Pierce, J. R. (2013, November). Large contribution of natural
 453 aerosols to uncertainty in indirect forcing. *Nature*, *503*(7474), 67–71. Re-
 454 trieved 2024-04-18, from <https://www.nature.com/articles/nature12674>
 455 (Publisher: Nature Publishing Group) doi: [10.1038/nature12674](https://doi.org/10.1038/nature12674)
- 456 Chen, Y., Haywood, J., Wang, Y., Malavelle, F., Jordan, G., Partridge, D., ...
 457 Lohmann, U. (2022, August). Machine learning reveals climate forcing from
 458 aerosols is dominated by increased cloud cover. *Nature Geoscience*, *15*(8),
 459 609–614. Retrieved from <https://doi.org/10.1038/s41561-022-00991-6>
 460 doi: [10.1038/s41561-022-00991-6](https://doi.org/10.1038/s41561-022-00991-6)
- 461 Chin, M., Ginoux, P., Kinne, S., Torres, O., Holben, B. N., Duncan, B. N., ...
 462 Nakajima, T. (2002). Tropospheric aerosol optical thickness from the
 463 gcart model and comparisons with satellite and sun photometer mea-
 464 surements. *J. Atmos. Sci.*, *59*(3), 461–483. Retrieved from [http://](http://dx.doi.org/10.1175/1520-0469(2002)059<0461:TAOTFT>2.0.CO;2)
 465 [dx.doi.org/10.1175/1520-0469\(2002\)059<0461:TAOTFT>2.0.CO;2](http://dx.doi.org/10.1175/1520-0469(2002)059<0461:TAOTFT>2.0.CO;2) doi:
 466 [10.1175/1520-0469\(2002\)059<0461:TAOTFT>2.0.CO;2](https://doi.org/10.1175/1520-0469(2002)059<0461:TAOTFT>2.0.CO;2)
- 467 Christensen, M. W., Gettelman, A., Cermak, J., Dagan, G., Diamond, M., Douglas,
 468 A., ... Yuan, T. (2022). Opportunistic experiments to constrain aerosol ef-
 469 fective radiative forcing. *Atmospheric Chemistry and Physics*, *22*(1), 641–674.
 470 Retrieved from <https://acp.copernicus.org/articles/22/641/2022/> doi:
 471 [10.5194/acp-22-641-2022](https://doi.org/10.5194/acp-22-641-2022)
- 472 Copernicus Climate Change Service. (2017). *ERA5: Fifth generation of ECMWF at-*
 473 *mospheric reanalyses of the global climate*. Retrieved from [http://doi.org/](http://doi.org/10.24381/cds.adbb2d47)
 474 [10.24381/cds.adbb2d47](https://doi.org/10.24381/cds.adbb2d47) (Copernicus Climate Change Service Climate Data

- 475 Store (CDS), last accessed May 11th 2021)
- 476 Denier van der Gon, H., Hendriks, C., Kuenen, J., Segers, A. A., & Visschedijk, A.
477 (2011). *Description of current temporal emission patterns and sensitivity of*
478 *predicted AQ for temporal emission patterns, TNO Report, EU FP7 MACC de-*
479 *liverable report D_DEMIS-1.3* (Tech. Rep.). Princetonlaan 6, 3584 CB Utrecht,
480 The Netherlands: TNO.
- 481 Dusek, U., Frank, G. P., Hildebrandt, L., Curtius, J., Schneider, J., Walter, S., ...
482 Andreae, M. O. (2006). Size matters more than chemistry for cloud-nucleating
483 ability of aerosol particles. *Science*, *312*(5778), 1375-1378. Retrieved from
484 <https://www.science.org/doi/abs/10.1126/science.1125261> doi:
485 10.1126/science.1125261
- 486 EEA. (2014). *Emission trends of sulphur oxides* [Data Visualization]. Retrieved
487 2024-04-17, from https://www.eea.europa.eu/data-and-maps/daviz/emission-trends-of-sulphur-oxides#tab-chart_1
- 488 Ekman, A. M. L. (2014). Do sophisticated parameterizations of aerosol-
489 cloud interactions in CMIP5 models improve the representation of re-
490 cent observed temperature trends? *Journal of Geophysical Research:*
491 *Atmospheres*, *119*(2), 817–832. Retrieved 2024-04-17, from <https://onlinelibrary.wiley.com/doi/abs/10.1002/2013JD020511> (eprint:
492 <https://onlinelibrary.wiley.com/doi/pdf/10.1002/2013JD020511>) doi:
493 10.1002/2013JD020511
- 494 Emmons, L. K., Walters, S., Hess, P. G., Lamarque, J.-F., Pfister, G. G., Fillmore,
495 D., ... Kloster, S. (2010). Description and evaluation of the Model for Ozone
496 and Related chemical Tracers, version 4 (MOZART-4). *Geoscientific Model*
497 *Development*, *3*(1), 43–67. doi: 10.5194/gmd-3-43-2010
- 498 Fiedler, S., van Noije, T., Smith, C. J., Boucher, O., Dufresne, J.-L., Kirkevåg, A.,
499 ... Schulz, M. (2023). Historical changes and reasons for model differences in
500 anthropogenic aerosol forcing in cmip6. *Geophysical Research Letters*, *50*(15),
501 e2023GL104848. Retrieved from [https://agupubs.onlinelibrary.wiley](https://agupubs.onlinelibrary.wiley.com/doi/abs/10.1029/2023GL104848)
502 [.com/doi/abs/10.1029/2023GL104848](https://agupubs.onlinelibrary.wiley.com/doi/abs/10.1029/2023GL104848) (e2023GL104848 2023GL104848) doi:
503 <https://doi.org/10.1029/2023GL104848>
- 504 Ghan, S. J., Leung, L. R., Easter, R. C., & Abdul-Razzak, H. (1997). Prediction
505 of cloud droplet number in a general circulation model. *Journal of Geophysi-*
506 *cal Research: Atmospheres*, *102*(D18), 21777-21794. Retrieved from <https://agupubs.onlinelibrary.wiley.com/doi/abs/10.1029/97JD01810> doi:
507 <https://doi.org/10.1029/97JD01810>
- 508 Grell, G. A., & Dévényi, D. (2002). A generalized approach to parameterizing con-
509 vection combining ensemble and data assimilation techniques. *Geophysical Re-*
510 *search Letters*, *29*(14), 38–1–38–4. doi: 10.1029/2002GL015311
- 511 Grell, G. A., Peckham, S. E., Schmitz, R., McKeen, S. A., Frost, G., Skamarock,
512 W. C., & Eder, B. (2005). Fully coupled “online” chemistry within
513 the wrf model. *Atmospheric Environment*, *39*(37), 6957-6975. Re-
514 trievied from <https://www.sciencedirect.com/science/article/pii/S1352231005003560> doi: <https://doi.org/10.1016/j.atmosenv.2005.04.027>
- 515 Gryspereidt, E., Povey, A. C., Grainger, R. G., Hasekamp, O., Hsu, N. C., Mulcahy,
516 J. P., ... Sorooshian, A. (2023). Uncertainty in aerosol–cloud radiative forcing
517 is driven by clean conditions. *Atmospheric Chemistry and Physics*, *23*(7),
518 4115–4122. Retrieved from [https://acp.copernicus.org/articles/23/](https://acp.copernicus.org/articles/23/4115/2023/)
519 [4115/2023/](https://acp.copernicus.org/articles/23/4115/2023/) doi: 10.5194/acp-23-4115-2023
- 520 Guenther, A. B., Jiang, X., Heald, C. L., Sakulyanontvittaya, T., Duhl, T., Em-
521 mons, L. K., & Wang, X. (2012). The Model of Emissions of Gases and
522 Aerosols from Nature version 2.1 (MEGAN2.1): an extended and updated
523 framework for modeling biogenic emissions. *Geoscientific Model Development*,
524 *5*(6), 1471–1492. doi: 10.5194/gmd-5-1471-2012
- 525 Hodnebrog, O., Myhre, G., Jouan, C., Andrews, T., Forster, P. M., Jia, H., ...

- 530 Schulz, M. (2024, April). Recent reductions in aerosol emissions have
 531 increased Earth’s energy imbalance. *Communications Earth & Environ-*
 532 *ment*, 5(1), 1–9. Retrieved 2024-04-17, from [https://www.nature.com/](https://www.nature.com/articles/s43247-024-01324-8)
 533 [articles/s43247-024-01324-8](https://www.nature.com/articles/s43247-024-01324-8) (Publisher: Nature Publishing Group) doi:
 534 10.1038/s43247-024-01324-8
- 535 Hubanks, P., Platnick, S., King, M., & Ridgway, B. (2016). *MODIS Atmosphere*
 536 *L3 Gridded Product Algorithm Theoretical Basis Document (ATBD) & Users*
 537 *Guide* (Tech. Rep.). NASA EOS.
- 538 Ilyinskaya, E., Schmidt, A., Mather, T. A., Pope, F. D., Witham, C., Baxter, P.,
 539 ... Edmonds, M. (2017). Understanding the environmental impacts of large
 540 fissure eruptions: Aerosol and gas emissions from the 2014–2015 holuhraun
 541 eruption (iceland). *Earth and Planetary Science Letters*, 472, 309–322. Re-
 542 trieved from [https://www.sciencedirect.com/science/article/pii/](https://www.sciencedirect.com/science/article/pii/S0012821X17302911)
 543 [S0012821X17302911](https://www.sciencedirect.com/science/article/pii/S0012821X17302911) doi: <https://doi.org/10.1016/j.epsl.2017.05.025>
- 544 Ioannidis, E., Law, K. S., Raut, J.-C., Marelle, L., Onishi, T., Kirpes, R. M., ...
 545 Pratt, K. A. (2023). Modelling wintertime sea-spray aerosols under arctic
 546 haze conditions. *Atmospheric Chemistry and Physics*, 23(10), 5641–5678. Re-
 547 trieved from <https://acp.copernicus.org/articles/23/5641/2023/> doi:
 548 10.5194/acp-23-5641-2023
- 549 IPCC. (2023). The earth’s energy budget, climate feedbacks and climate sensitivity.
 550 In *Climate change 2021 – the physical science basis: Working group i contri-*
 551 *bution to the sixth assessment report of the intergovernmental panel on climate*
 552 *change* (p. 923–1054). Cambridge University Press.
- 553 Lana, A., Bell, T. G., Simó, R., Vallina, S. M., Ballabrera-Poy, J., Kettle, A. J., ...
 554 Liss, P. S. (2011). An updated climatology of surface dimethylsulfide concen-
 555 trations and emission fluxes in the global ocean. *Global Biogeochemical Cycles*,
 556 25(1). doi: 10.1029/2010GB003850
- 557 Lapere, R., Thomas, J. L., Marelle, L., Ekman, A. M. L., Frey, M. M., Lund,
 558 M. T., ... Zieger, P. (2023). The representation of sea salt aerosols
 559 and their role in polar climate within cmip6. *Journal of Geophysical Re-*
 560 *search: Atmospheres*, 128(6), e2022JD038235. Retrieved from [https://](https://agupubs.onlinelibrary.wiley.com/doi/abs/10.1029/2022JD038235)
 561 agupubs.onlinelibrary.wiley.com/doi/abs/10.1029/2022JD038235
 562 (e2022JD038235 2022JD038235) doi: <https://doi.org/10.1029/2022JD038235>
- 563 Li, G., Wieder, J., Pasquier, J. T., Henneberger, J., & Kanji, Z. A. (2022). Predict-
 564 ing atmospheric background number concentration of ice-nucleating particles
 565 in the arctic. *Atmospheric Chemistry and Physics*, 22(21), 14441–14454. Re-
 566 trieved from <https://acp.copernicus.org/articles/22/14441/2022/> doi:
 567 10.5194/acp-22-14441-2022
- 568 Lohmann, U., & Feichter, J. (2005, March). Global indirect aerosol effects: a re-
 569 view. *Atmospheric Chemistry and Physics*, 5(3), 715–737. Retrieved 2024-04-
 570 17, from <https://acp.copernicus.org/articles/5/715/2005/> (Publisher:
 571 Copernicus GmbH) doi: 10.5194/acp-5-715-2005
- 572 Lohmann, U., Feichter, J., Penner, J., & Leaitch, R. (2000). Indirect effect of sul-
 573 fate and carbonaceous aerosols: A mechanistic treatment. *Journal of Geophys-*
 574 *ical Research: Atmospheres*, 105(D10), 12193–12206. Retrieved from [https://](https://agupubs.onlinelibrary.wiley.com/doi/abs/10.1029/1999JD901199)
 575 agupubs.onlinelibrary.wiley.com/doi/abs/10.1029/1999JD901199 doi:
 576 <https://doi.org/10.1029/1999JD901199>
- 577 Lohmann, U., Lüönd, F., & Mahrt, F. (2016). *An Introduction to Clouds: From*
 578 *the Microscale to Climate*. Cambridge: Cambridge University Press. Re-
 579 trieved 2024-04-17, from [https://www.cambridge.org/core/books/](https://www.cambridge.org/core/books/an-introduction-to-clouds/F5A8096E7A3BD5C8FFD9208248DD1839)
 580 [an-introduction-to-clouds/F5A8096E7A3BD5C8FFD9208248DD1839](https://www.cambridge.org/core/books/an-introduction-to-clouds/F5A8096E7A3BD5C8FFD9208248DD1839) doi:
 581 10.1017/CBO9781139087513
- 582 Madeleine, J.-B., Hourdin, F., Grandpeix, J.-Y., Rio, C., Dufresne, J.-L., Vignon,
 583 E., ... Bonazzola, M. (2020). Improved representation of clouds in the
 584 atmospheric component lmdz6a of the ipsl-cm6a earth system model. *Jour-*

- 585 *nal of Advances in Modeling Earth Systems*, 12(10), e2020MS002046. Retrieved from <https://agupubs.onlinelibrary.wiley.com/doi/abs/10.1029/2020MS002046> (e2020MS002046 10.1029/2020MS002046) doi: <https://doi.org/10.1029/2020MS002046>
- 586
587
588
- 589 Malavelle, F. F., Haywood, J. M., Jones, A., Gettelman, A., Clarisse, L., Bauduin,
590 S., ... Thordarson, T. (2017, June). Strong constraints on aerosol–cloud in-
591 teractions from volcanic eruptions. *Nature*, 546(7659), 485–491. Retrieved
592 2024-04-17, from <https://www.nature.com/articles/nature22974> (Pub-
593 lisher: Nature Publishing Group) doi: 10.1038/nature22974
- 594 Marelle, L., Raut, J.-C., Law, K. S., Berg, L. K., Fast, J. D., Easter, R. C., ...
595 Thomas, J. L. (2017). Improvements to the wrf-chem 3.5.1 model for quasi-
596 hemispheric simulations of aerosols and ozone in the arctic. *Geoscientific Model*
597 *Development*, 10(10), 3661–3677. Retrieved from [https://gmd.copernicus](https://gmd.copernicus.org/articles/10/3661/2017/)
598 [.org/articles/10/3661/2017/](https://gmd.copernicus.org/articles/10/3661/2017/) doi: 10.5194/gmd-10-3661-2017
- 599 Müllenstädt, J., & Feingold, G. (2018, March). The Radiative Forcing of
600 Aerosol–Cloud Interactions in Liquid Clouds: Wrestling and Embracing
601 Uncertainty. *Current Climate Change Reports*, 4(1), 23–40. Retrieved
602 2024-04-18, from <https://doi.org/10.1007/s40641-018-0089-y> doi:
603 10.1007/s40641-018-0089-y
- 604 Nightingale, P. D., Malin, G., Law, C. S., Watson, A. J., Liss, P. S., Liddi-
605 coat, M. I., ... Upstill-Goddard, R. C. (2000). In situ evaluation of air-
606 sea gas exchange parameterizations using novel conservative and volatile
607 tracers. *Global Biogeochemical Cycles*, 14(1), 373–387. Retrieved from
608 <http://dx.doi.org/10.1029/1999GB900091> doi: 10.1029/1999GB900091
- 609 Pfeffer, M. A., Bergsson, B., Barsotti, S., Stefánsdóttir, G., Galle, B., Arellano, S.,
610 ... Mereu, L. (2018). Ground-based measurements of the 2014–2015 holuhraun
611 volcanic cloud (iceland). *Geosciences*, 8(1). Retrieved from [https://](https://www.mdpi.com/2076-3263/8/1/29)
612 www.mdpi.com/2076-3263/8/1/29 doi: 10.3390/geosciences8010029
- 613 Quaas, J., Arola, A., Cairns, B., Christensen, M., Deneke, H., Ekman, A. M. L., ...
614 Wendisch, M. (2020). Constraining the twomey effect from satellite observa-
615 tions: issues and perspectives. *Atmospheric Chemistry and Physics*, 20(23),
616 15079–15099. Retrieved 2024-04-17, from [https://acp.copernicus.org/](https://acp.copernicus.org/articles/20/15079/2020/)
617 [articles/20/15079/2020/](https://acp.copernicus.org/articles/20/15079/2020/) (Publisher: Copernicus GmbH) doi:
618 10.5194/acp-20-15079-2020
- 619 Quaas, J., Jia, H., Smith, C., Albright, A. L., Aas, W., Bellouin, N., ... Schulz, M.
620 (2022). Robust evidence for reversal of the trend in aerosol effective climate
621 forcing. *Atmospheric Chemistry and Physics*, 22(18), 12221–12239. Retrieved
622 from <https://acp.copernicus.org/articles/22/12221/2022/> doi:
623 10.5194/acp-22-12221-2022
- 624 Seinfeld, J. H., Bretherton, C., Carslaw, K. S., Coe, H., DeMott, P. J., Dunlea,
625 E. J., ... Wood, R. (2016). Improving our fundamental understanding
626 of the role of aerosol-cloud interactions in the climate system. *Proceed-*
627 *ings of the National Academy of Sciences*, 113(21), 5781–5790. Retrieved
628 from <https://www.pnas.org/doi/abs/10.1073/pnas.1514043113> doi:
629 10.1073/pnas.1514043113
- 630 Tegen, I., Hollrig, P., Chin, M., Fung, I., Jacob, D., & Penner, J. (1997). Con-
631 tribution of different aerosol species to the global aerosol extinction opti-
632 cal thickness: Estimates from model results. *Journal of Geophysical Re-*
633 *search: Atmospheres*, 102(D20), 23895–23915. Retrieved from [https://](https://agupubs.onlinelibrary.wiley.com/doi/abs/10.1029/97JD01864)
634 agupubs.onlinelibrary.wiley.com/doi/abs/10.1029/97JD01864 doi:
635 <https://doi.org/10.1029/97JD01864>
- 636 Thompson, G., & Eidhammer, T. (2014). A study of aerosol impacts on clouds
637 and precipitation development in a large winter cyclone. *Journal of the*
638 *Atmospheric Sciences*, 71(10), 3636 - 3658. Retrieved from [https://](https://journals.ametsoc.org/view/journals/atsc/71/10/jas-d-13-0305.1.xml)
639 journals.ametsoc.org/view/journals/atsc/71/10/jas-d-13-0305.1.xml

- doi: 10.1175/JAS-D-13-0305.1
- 640
641 Tilmes, S., Emmons, L., Buchholz, R., & Team, T. C. D. (2022). [data set]
642 *cesm2.2/cam-chem output for boundary conditions. ucar/ncar - atmospheric*
643 *chemistry observations and modeling laboratory*. (Accessed 01 FEB 2024) doi:
644 <https://doi.org/10.5065/XS0R-QE86>
- 645 Twomey, S. (1974, December). Pollution and the planetary albedo. *Atmospheric*
646 *Environment (1967)*, 8(12), 1251–1256. Retrieved 2024-03-19, from [https://](https://www.sciencedirect.com/science/article/pii/0004698174900043)
647 www.sciencedirect.com/science/article/pii/0004698174900043 doi: 10
648 .1016/0004-6981(74)90004-3
- 649 von Glasow, R., & Crutzen, P. J. (2004). Model study of multiphase dms oxidation
650 with a focus on halogens. *Atmospheric Chemistry and Physics*, 4(3), 589–608.
651 Retrieved from <https://acp.copernicus.org/articles/4/589/2004/> doi:
652 10.5194/acp-4-589-2004
- 653 von Salzen, K., Whaley, C. H., Anenberg, S. C., Van Dingenen, R., Klimont, Z.,
654 Flanner, M. G., ... Winter, B. (2022, October). Clean air policies are key
655 for successfully mitigating Arctic warming. *Communications Earth & Envi-*
656 *ronment*, 3(1), 1–11. Retrieved 2024-03-19, from [https://www.nature.com/](https://www.nature.com/articles/s43247-022-00555-x)
657 [articles/s43247-022-00555-x](https://www.nature.com/articles/s43247-022-00555-x) (Publisher: Nature Publishing Group) doi:
658 10.1038/s43247-022-00555-x
- 659 Wiedinmyer, C., Yokelson, R. J., & Gullett, B. K. (2014). Global Emissions of Trace
660 Gases, Particulate Matter, and Hazardous Air Pollutants from Open Burning
661 of Domestic Waste. *Environmental Science & Technology*, 48(16), 9523–9530.
662 doi: 10.1021/es502250z
- 663 Xu, K.-M., & Randall, D. A. (1996). A semiempirical cloudiness parameteriza-
664 tion for use in climate models. *Journal of Atmospheric Sciences*, 53(21), 3084
665 - 3102. Retrieved from [https://journals.ametsoc.org/view/journals/](https://journals.ametsoc.org/view/journals/atsc/53/21/1520-0469_1996_053_3084_ascpfu_2_0_co_2.xml)
666 [atsc/53/21/1520-0469_1996_053_3084_ascpfu_2_0_co_2.xml](https://journals.ametsoc.org/view/journals/atsc/53/21/1520-0469_1996_053_3084_ascpfu_2_0_co_2.xml) doi: 10.1175/
667 1520-0469(1996)053(3084:ASCPFU)2.0.CO;2
- 668 Zaveri, R. A., Easter, R. C., Fast, J. D., & Peters, L. K. (2008). Model for Simu-
669 lating Aerosol Interactions and Chemistry (MOSAIC). *Journal of Geophysical*
670 *Research: Atmospheres*, 113(D13). doi: 10.1029/2007JD008782
- 671 Zelinka, M. D., Smith, C. J., Qin, Y., & Taylor, K. E. (2023). Comparison of
672 methods to estimate aerosol effective radiative forcings in climate mod-
673 els. *Atmospheric Chemistry and Physics*, 23(15), 8879–8898. Retrieved
674 from <https://acp.copernicus.org/articles/23/8879/2023/> doi:
675 10.5194/acp-23-8879-2023